


## PAPER

# Black pepper and piperine induce anticancer effects on leukemia cell line

Somesh Banerjee,<sup>1</sup> Parul Katiyar,<sup>1</sup> Vijay Kumar,<sup>2</sup> Shashank Sagar Saini,<sup>3</sup> Ritu Varshney,<sup>1</sup> Vengadesan Krishnan,<sup>2</sup> Debabrata Sircar<sup>3</sup> and Partha Roy <sup>1,\*</sup>

<sup>1</sup>Molecular Endocrinology Laboratory, Department of Biotechnology, Indian Institute of Technology Roorkee, Roorkee 247667, Uttarakhand, India, <sup>2</sup>Laboratory of Structural Microbiology, Regional Centre for Biotechnology, Faridabad 121001, Haryana, India and <sup>3</sup>Plant Molecular Biology Laboratory, Department of Biotechnology, Indian Institute of Technology Roorkee, Roorkee 247667, Uttarakhand, India

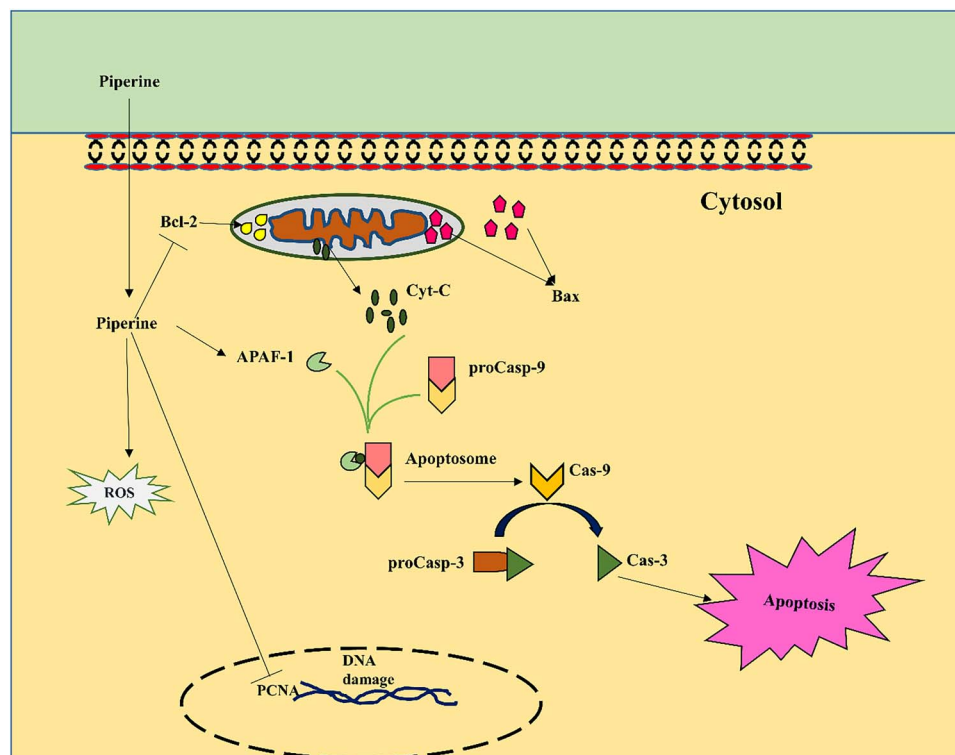
\*Correspondence address. Molecular Endocrinology Laboratory, Department of Biotechnology, Indian Institute of Technology Roorkee, Roorkee 247667, Uttarakhand, India. E-mail: partha.roy@bt.iitr.ac.in

## Abstract

The black pepper, most commonly used in Indian cuisines for ages, is considered as “king of spices.” The present study evaluates the anticancer potential of black pepper and its main constituent, i.e. alkaloid piperine, against human leukemia cell line, K-562 cells. Gas chromatography–mass spectrometry (GC–MS) analysis confirmed the presence of piperine in black pepper extract. The methanolic extract of black pepper (BP-M) and pure piperine (PIP) showed a strong cytotoxic effect against this cell line. Both BP-M and PIP generated apoptotic bodies in K-562 cells and caused nuclear condensation as visualized by fluorescent microscopy, which was further confirmed by flow cytometry analysis. BP-M and PIP also generated reactive oxygen species in K-562 cells as established by flow cytometry. The translation of Bax, caspase-3 and caspase-9 genes was found to be upregulated with subsequent downregulation of Bcl-2 gene. The anti-proliferative effect of both BP-M and PIP was also observed by trypan blue staining and was further confirmed by the downregulated expression of proliferating cell nuclear antigen (PCNA). The molecular docking studies showed the binding of PIP with PCNA and Bcl-2 and supported the *in vitro* findings. The docking studies also proposed the binding of PIP to ADP binding pocket of Apaf-1 protein. Taken together, these findings signify the anticancer potential of both black pepper and PIP, thus proposing black pepper as a potent nutraceutical for preventing the progression of chronic myeloid leukemia.

**Key words:** black pepper, piperine, chronic myeloid leukemia, intrinsic apoptosis pathway, reactive oxygen species

## Graphical Abstract



## Introduction

Cancer has emerged as a significant health problem globally, affecting both developed and underdeveloped countries [1]. Cancer is the second leading cause of human death after heart disease. Among all other cancers, leukemia represents a fatal hematological malignancy, a cancer of the blood and bone marrow, which alone claims 0.62% death annually [2]. Human chronic myeloid leukemia (CML) is a common type of leukemia, generated due to t(9;22)(q34;11) chromosomal translocation [3]. This translocation generates oncogenic BCR-ABL tyrosine kinase fusion protein, which remains confined to cell cytoplasm, while the wild-type ABL protein shuttles between nucleus and cytoplasm [4]. This tyrosine kinase protein leads to aberrant phosphorylation of several substrates of different intracellular pathways [5].

The first-line treatment of CML involves tyrosine kinase inhibitor, namely imatinib, which was introduced 10 years back. Later dasatinib, nilotinib and bosutinib were also tested clinically. However, due to mutation in the ABL kinase domains, many patients developed resistance to these drugs [6]. The difficulty in the current time for CML therapy has led to the discovery and development of approaches based on traditional medicines, which are supposed to possess lower side effects than existing therapeutics.

Health care of ~80% of the world's population relies mainly on traditional medicines [7]. Several medicinal plant products have been proven to aid in various ailments successfully. Black pepper plays a very conspicuous role in the Indian system of medicines—*Ayurveda*, *Sidha* and *Unani*, being a vital ingredient of different medicinal formulations used in these practices. Black pepper, considered as “king of spices,” is the most traded spice variety across the globe. The essential commercial part

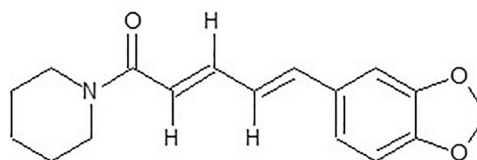


Figure 1: chemical structure of piperine

of black pepper plant is its dried and matured fruit, which is popular for its particular aroma and flavor because of the presence of volatile oils and major alkaloid, i.e. piperine, which constitutes about 2.8–17.3 mg per gram of dried black pepper. The structure of piperine consists of piperidine linked to 3,4-methylenedioxyphenyl moiety by the C5 amide bridge (Fig. 1). Black pepper has been known to have bactericidal, insecticidal, antidiarrheal, antispasmodic and anticancer properties [8]. Piperine has also been reported to have immune-modulatory, antidepressant, anti-inflammatory and anti-diabetic and anticancer properties [9].

In previous studies, it has been reported that piperine, a major metabolite of *Piper nigrum*, responded as a prominent anticancer agent [10–13]. However, to the best of our knowledge, the potential of black pepper and piperine has not been investigated in the condition of leukemia to date. Therefore, the main objective of this study was to explore the anticancer potential of black pepper and piperine against leukemia cell line i.e., K-562 cells.

## Materials and Methods

### Plant material and extraction

The matured fruit (peppercorn) of black pepper was procured from local herbal product stores of Roorkee, Uttarakhand, India,

who are engaged in making various traditional herbal formulations. The crushed powder of black pepper fruits was extracted with three different solvents: methanol (BP-M), ethanol (BP-E) and water (BP-Aq) (1:5, w/v) thrice independently. All the samples were stored at  $-80^{\circ}\text{C}$  until used. The extract supernatant was evaporated under vacuum at room temperature to dryness as dark brown mass using a vacuum concentrator (Eppendorf Concentrator plus™, Eppendorf, Hamburg, Germany). The dried extract was then reconstituted in dimethyl sulfoxide (DMSO, Cat. No. TC185, Himedia, Mumbai, India) and filtered (0.22  $\mu\text{m}$  filter, Axiva Sicheem Biotech, Haryana, India) before use in cell culture analysis. Piperine (PIP) (Cat. No. P49007, Sigma, St. Louis, MO, USA) was also dissolved in DMSO and filtered before use [14]. Both were used at 0.1% v/v ratio in the analysis [15].

### Estimation of total phenolic and total flavonoid contents

The total phenolic content of all three extracts (BP-M, BP-E and BP-Aq) was determined using the Folin–Ciocalteu method [16]. In brief, 200  $\mu\text{l}$  of the extract was mixed with 500  $\mu\text{l}$  of Folin–Ciocalteu reagent (1:9 dilutions with water) (Cat. No. 10822, Himedia, Mumbai, India) followed by 5-min incubation at room temperature. Then, 300  $\mu\text{l}$  of sodium carbonate (5% solution) was added and the solution was incubated further for 20 min at room temperature in dark condition. The absorbance was measured at 765 nm using FLUOstar Omega (BMG Labtech, Ortenberg, Germany) microplate reader. Gallic acid (Cat. No. G7384, Sigma, St. Louis, MO, USA) was used as the internal standard and total phenolic content was expressed as micrograms of gallic acid equivalents per gram dry mass (GAE). The total flavonoid content of all three extracts was measured by  $\text{AlCl}_3$  method [16]. In brief, 500  $\mu\text{l}$  of the extract was mixed with 500  $\mu\text{l}$  of aluminum chloride (2%) solution (Cat. No. MB054, Himedia, Mumbai, India) in ethanol and incubated for 1 h at room temperature. Then, the absorbance was measured at 420 nm using FLUOstar Omega (BMG Labtech, Ortenberg, Germany) microplate reader. Quercetin (Cat. No. Q4951, Sigma, St. Louis, MO, US) was used as internal standard and the total flavonoid content was expressed as micrograms of quercetin equivalent per gram dry mass (QE).

### Gas chromatography–mass spectrometry analysis

Gas chromatography–mass spectrometry (GC–MS) analysis was performed to separate and identify the metabolites present in three different extracts. For GC–MS analysis, 500  $\mu\text{l}$  of extract was first mixed with 50  $\mu\text{l}$  of internal standard, 2-phenylphenol (from 2 mg/ml in methanol stock) (Cat. No. P28263, Sigma, St. Louis, MO, USA). The mixture was then dried in a vacuum concentrator (Eppendorf Concentrator plus™, Eppendorf, Hamburg, Germany). The dried mass was directly derivatized with 70  $\mu\text{l}$  of N-Methyl-N-(trimethylsilyl) trifluoroacetamide (MSTFA) (Cat. No. M-132 Superlo, Sigma, St. Louis, MO, USA) at  $37^{\circ}\text{C}$  for 60 min, followed by centrifugation at  $14\,000 \times g$  for 10 min [17]. The resulting supernatant was taken out in a GC glass vial and immediately analyzed by GC–MS. PIP was used as standard control and similar derivatization was performed. The GC–MS analysis was performed on Agilent 7890B gas chromatograph coupled with Agilent 8977C mass detector (Agilent Technologies, Santa Clara, CA, USA). HP-5 MS column [5% Phenyl Methyl Polysiloxane: 30 m  $\times$  0.25 mm (I.D.)  $\times$  0.25  $\mu\text{m}$ ] was used for metabolite separation with helium as a carrier gas with a flow rate of 1 ml/min. The injection volume was 1  $\mu\text{l}$  with split-less mode. The injector temperature was set at  $280^{\circ}\text{C}$ . The oven temperature was initially set at  $70^{\circ}\text{C}$  for 2 min, then ramped to  $220^{\circ}\text{C}$  at a rate of  $10^{\circ}\text{C}/\text{min}$  and then

further increased to  $310^{\circ}\text{C}$  at the rate of  $20^{\circ}\text{C}/\text{min}$  and then hold for 14 min at  $310^{\circ}\text{C}$ . The mass spectrometer (MS) operation parameters were set as follows: MS quad temperature  $150^{\circ}\text{C}$ , ion source temperature  $230^{\circ}\text{C}$ , electron energy (70 eV) and mass spectra collection range of 40–1000 m/z. Each sample was replicated three times. The metabolites were identified by matching the mass spectra of target metabolites with library search (Wiley; National Institute of Standards & Technology library- NIST 17). PIP was quantified using an authentic standard.

### Cell culture

The human bone marrow origin leukemia cell line, K-562 cells, was procured from the National Centre for Cell Science (Pune, India) and maintained in RPMI-1640 media (Cat. No. AT-162, Himedia, Mumbai, India). The normal human lung fibroblast cell line, MRC-5, was a kind gift from Dr. Hemant K. Gautam (Council of Scientific and Industrial Research-Institute of Genomics and Integrative Biology, New Delhi, India). The MRC-5 cell line was maintained in Eagle's Minimum Essential Medium (Cat. No. AT-154, Himedia, Mumbai, India). The cell culture media was supplemented with 10% fetal bovine serum (Cat. No. 11573397) and 100-U/ml penicillin–streptomycin and 100-mg/ml ampicillin mixture (Cat. No. 15240062, both from Gibco, Thermo Fisher Scientific, Waltham, MA, USA), and the cells were cultured in a humidified incubator at  $37^{\circ}\text{C}$  with 5%  $\text{CO}_2$ .

### Cytotoxic activity

The cytotoxic effect of black pepper and PIP on K-562 cells were measured using MTT [3-(4,5-dimethylthiazol-2-yl)-2,5-diphenyl tetrazolium bromide] assay [18]. All three black pepper extracts, i.e. BP-M, BP-E, BP-Aq and PIP, were tested three independent times. Briefly, 96-well plates were seeded with 200  $\mu\text{l}$  of media containing 5000 cells with various concentrations of black pepper extracts (50, 100 and 200  $\mu\text{g}/\text{ml}$ ) or PIP (25, 50 and 100  $\mu\text{M}$ ). The DMSO-treated cells were considered as control. The cells were incubated for 24 and 48 h. After the incubation, 20  $\mu\text{l}$  of MTT dye (Cat. No. TC191, Himedia, Mumbai, India) was supplemented to each well and the cells were incubated at  $37^{\circ}\text{C}$  for another 4 h. Then, after pipetting out the media, each well was replaced with 200  $\mu\text{l}$  of DMSO to dissolve the formazan crystal formed. The absorbance of the lysate was then measured at 570 nm using FLUOstar Omega (BMG Labtech, Ortenberg, Germany) microplate reader. The inhibition percentage was calculated as follows:

$$100 - \left[ \frac{\text{Mean absorbance of phytochemical treated cells}}{\text{Mean absorbance of vehicle-treated cells}} \times 100 \right]$$

The  $\text{IC}_{25}$  and  $\text{IC}_{50}$  values were evaluated on the basis of inhibition percentage values using Graph Pad Prism 6.01 software (San Diego, CA, USA).

### Cellular staining

In order to visualize changes in nuclear status and formation of apoptotic bodies, the K-562 cells were visualized after performing dual Acridine Orange/Ethidium Bromide (AO/EB) staining [19]. Briefly, the cells were treated at  $\text{IC}_{50}$  concentration of both BP-M and PIP for 48 h. Then, the cells were harvested and washed twice with PBS and incubated with dye mixture (AO and EB, both 100  $\mu\text{g}/\text{ml}$  in PBS, Cat. No. 318337 and E8751, respectively, Sigma, St. Louis, MO, USA) and observed under a fluorescence microscope (Zeiss, Axiovert 25, Germany).

The nuclear morphology of K-562 cells under similar treatment conditions was also visualized by performing Hoechst staining [20]. Briefly, the treated cells were harvested, washed twice with PBS and incubated for 15 min with 100 ng/ml of Hoechst 33342 dye (Cat. No. TC266, Himedia, Mumbai, India) in PBS. Then, the stained cells were observed under a fluorescent microscope (EVOS® FL Cell Imaging System, Thermo Fischer Scientific, Waltham, MA, USA). The observations were performed three independent times.

### Trypan blue dye exclusion assay

The anti-proliferative effect of BP-M and PIP was examined by manual counting of cells after staining them with trypan blue [21]. Briefly, K-562 cells were treated with BP-M and PIP at IC<sub>25</sub> and IC<sub>50</sub> concentrations for 48 h, respectively. The K-562 cells treated with DMSO were considered as control. Then, the cells were stained with trypan blue dye (Cat. No. GRM263, Himedia, Mumbai, India) and counted manually using a hemocytometer.

### Flow cytometry assay for measurement of intracellular reactive oxygen species levels

The intracellular accumulation of reactive oxygen species (ROS) was determined by performing flow cytometry analysis using a fluorescence-activated cell sorter (FACS Calibur, BD Biosciences, San Jose, CA, USA), as mentioned previously [22]. Briefly, K-562 cells were treated at IC<sub>25</sub> and IC<sub>50</sub> equivalent concentrations of BP-M and PIP, respectively, for 48 h. The H<sub>2</sub>O<sub>2</sub> treated cells were considered as a positive control for this analysis. Then, the cells were harvested and washed twice with PBS followed by staining for 30 min with 2 μM concentration of 2', 7'-dichlorodihydrofluorescein diacetate, acetyl ester (DCFDA) (Cat. No. D6883, Sigma, St. Louis, MO, USA) at room temperature in dark condition. Then, the fluorescence intensity of cell suspension was analyzed immediately at 530 nm (FL-1 channel).

### Annexin-PI flow cytometry assay for induction of apoptosis

Black pepper and PIP-induced apoptosis in K-562 cells were determined quantitatively using Annexin V-conjugated Alexa Fluor 488 apoptosis assay kit (ThermoFischer Scientific, Waltham, MA, USA) following the manufacturer's instructions. Briefly, after 48 h treatment of cells with BP-M, PIP (IC<sub>25</sub> and IC<sub>50</sub> values) and DMSO (control), the cells were harvested and washed twice with PBS. The cells were then incubated for staining with Annexin V AlexaFluor 488 and propidium iodide (PI) in binding buffer at room temperature for 15 min in dark. The cells were then analyzed on a fluorescence-activated cell sorter (FACS Calibur, BD Biosciences, San Jose, CA, USA), and the data were analyzed using software Cell Quest 3.3.

### Gene expression analysis

Total RNA from K-562 cells treated at IC<sub>25</sub> and IC<sub>50</sub> equivalent concentrations of BP-M and PIP (48 h), respectively, or with DMSO (control) were isolated using RNA isolation reagent as per the instructions of manufacturers (RNA X-Press Reagent, Himedia, Mumbai, India). The RNA samples were then quantified, and

the first-strand cDNA was synthesized using 2 μg RNA samples. The primers for caspase-3, caspase-9, Bax, Bcl-2, proliferating cell nuclear antigen (PCNA) and β-actin genes were designed using Primer3 software (Whitehead Institute for Biomedical Research, Cambridge, MA, USA) and the details of primer sequences and PCR conditions are depicted in Table 1. Finally, the PCR products were separated on 2% agarose gel and visualized in a gel documentation system (BioRad, Hercules, CA, USA). The intensity of the bands on gels was analyzed using ImageJ 1.52a software (NIH, Bethesda, MD, USA). The entire procedure was carried out three independent times.

The expression of caspase-3, caspase-9 and PCNA was also evaluated by quantitative real-time PCR (RT-qPCR) analysis. The primer sequence for the genes are listed in Table 1. RT-qPCR was performed using SYBR green master mix (PowerUp™ SYBR™ Green Master mix, Applied Biosystems, Thermo Fischer Scientific, Waltham, MA, USA, Cat. No. A25742) using an RT-qPCR equipment (Applied Biosystems™ QuantStudio™ 5, ThermoFischer Scientific, Waltham, MA, USA). The amount of PCR product for the gene of interest in different treatment conditions was compared with the amount of β-actin produced to estimate the variations. The entire procedure was carried out three independent times. The relative expression of mRNA of test genes were calculated using the comparative 2<sup>-ΔΔ</sup> method [23].

### Western blotting analysis

Total protein of K-562 cells treated at IC<sub>25</sub> and IC<sub>50</sub> concentration of BP-M and PIP (48 h), respectively, or DMSO (control) was isolated with RIPA lysis buffer (Cat. No. TC131, Himedia, Mumbai, India) supplemented with 1X protease inhibitor cocktail (Cat. No. ML051, Himedia, Mumbai, India). The isolated protein was quantified with a BCA protein estimation kit (Cat. No. 71285-M, Sigma, St. Louis, MO, USA). The immunoblot analysis was performed, as mentioned elsewhere. Briefly, 40 μg of protein samples were analyzed on 10% polyacrylamide gels, then transferred to PVDF membrane and were blocked using 3% BSA in TBS-T buffer for 2 h. Then, the membrane was incubated (4°C, overnight) with primary anti-caspase-3, caspase-9, Bax, Bcl-2, PCNA and GAPDH antibodies (1:1000) (all from Elabsciences, Houston, TX, USA) in 3% BSA. After this step, the membranes were washed and incubated with horseradish peroxidase-conjugated secondary anti-rabbit or anti-mouse antibody (1:10,000) (Santa Cruz Biotechnology Inc., Dallas, TX, USA). The chemiluminescence was developed using ECL reagent (BioRad, CA, USA) and captured on X-ray films. The densitometric analyses of blots were performed by ImageJ 1.52a software (NIH, Bethesda, MD, USA) using GAPDH as an internal control.

### Molecular docking study

The binding of PIP, the principal constituent of black pepper, with different proteins of apoptotic signaling pathway was assessed by performing molecular docking analysis using AutoDock version 4.2 software [24]. The target proteins selected for this study were (i) Bcl-2 family of protein, (ii) apoptotic protease-activating factor 1 (Apaf-1) and (iii) cellular proliferation factor, PCNA. Among the Bcl-2 family, the crystal structure of anti-apoptotic protein (human Bcl-2) in complex with N-heteroaryl sulfonamide inhibitor (PDB ID: 4IEH, Resolution 2.10 Å) was used for docking calculation with PIP [25]. For docking calculation of PIP with PCNA and Apaf-1, the crystal structure of PCNA in complex with T2AA (PDB ID: 3WGW, Resolution

**Table 1:** details of oligonucleotide primer sequences used in this study for PCR

Name of gene	Forward primer sequence (5'-3')	Reverse primer sequence (5'-3')	Product size (bp)	Annealing temp (°C)
Caspase-3 (>NM_004346.4)	GGTTCATCCAGTCGCTTTGTG	GCGTCAAAGGAAAAGGACTCA	121	60.0
Caspase-9 (>NM_001229.5)	AGGCCCATATGATCGAGGA	GGCCTGTGTCCTCTAAGCAG	139	60.3
Bax (>NM_138763.4)	CCTGTGCACCAAGGTGCCGGAAGT	CCACCCTGGTCTTGGATCCAGCCC	99	68.2
Bcl-2 (>NM_000657.3)	TTGTGGCCTTCTTTGAGTTCGGTG	GGTGCCGGTTCAGGTACTCAGTCA	114	60.9
PCNA (>NM_002592.2)	GTTACTGAGGGCCGAGAAGCG	GCCGGAAGGAGGAAACTCT	167	61.3
$\beta$ -Actin (>NM_001101.5)	TCACCCACACTGTGCCCATCTACGA	CAGCGGAACCGCTCATTGCCAATGG	296	65.0
$\beta$ -Actin (>NM_001101.5) (RT-qPCR)	TACGCCAACACAGTGTCTGTCT	CTGCATCTGTCCGCAATG	63	60.0

2.80 Å) [26], and crystal structure of Apaf-1 with ADP (PDB ID: 1Z6T Resolution 2.21 Å) [27], were used, respectively. ADT tools was used for ligand and protein preparations. The grid maps were prepared using 60 × 60 × 60 grid points with 0.375 Å spacing in x, y and z directions centered at the active sites of individual macromolecules. Autogrid4 and autodock4 programs were used for calculating energy maps and docking of PIP, respectively. One hundred docked structures, i.e. 100 runs, were generated using Lamarckian Genetic Algorithm. All the generated binding poses of PIP with different proteins were ranked and clustered according to their root mean-square deviation (RMSD) values and binding affinities scores. Docked conformations were converted into PDBQT [Protein Data Bank, Partial Charge (Q) and Atom Type (T)] format and then analyzed. Chimera tool was used for visualization and figure generations [28].

### Statistical analysis

All data were represented as mean ± SEM. The difference among set conditions was evaluated by performing a one-way analysis of variance (ANOVA) test followed by the Bonferroni *post hoc* test using Graph Pad Prism 6.01 software (San Diego, CA, USA). The analyzed data with P-value <0.05 were considered statistically significant.

## Results

### Phytochemical evaluation of black pepper

The phytochemical composition of three black pepper extracts (BP-M, BP-E and BP-Aq) was evaluated. The total phenolics and flavonoids contents were estimated and are depicted in Table 2. As shown in Table 2, the total phenolic and flavonoid content in all three extracts were found to be around 50 GAE and 90 QE, respectively. The analysis confirmed that black pepper is a rich source of phenolic and flavonoid compounds. In the next phase, the GC-MS analysis revealed the presence of 44 different metabolites in all three extracts at varying concentrations. The metabolite contents were measured in terms of equivalent of internal standard ( $\mu$ g phenyl phenol/g dry weight) (Table 3). The representative total ion chromatogram of BP-M, BP-E, BP-Aq and PIP is shown in the supplementary figures (Figs S1 and S2). The presence of PIP in all three extracts was quantified by comparing the area of PIP in the extracts with the standard PIP obtained commercially (Sigma, St Louis, MO, USA). It was found that BP-M, BP-E and BP-Aq contained 0.78, 0.67 and 0.032 ng/mg dry weight of PIP, respectively (Table S1).

### Black pepper and piperine induce potent cytotoxic effect against K-562 cell line

The cytotoxic effect of black pepper was initially evaluated on K-562 cell line by MTT assay. Three different extracts of black pepper (BP-M, BP-E and BP-Aq) were investigated for their potential cytotoxic effects. The results confirmed the inhibition of cell viability by BP-M (Fig. 2a and e), BP-E (Fig. 2b and f) and BP-Aq (Fig. 2c and g) at both 24 and 48 h of treatment, albeit with high efficacy at a later hour. It is evident from the above data that at 200  $\mu$ g/ml concentration, all the extracts showed less than 50% cell viability ( $P < 0.05$ ). However, among all the tested extracts, BP-M showed the most significant cytotoxicity. This is based on the fact that 48 h of treatment with 200  $\mu$ g/ml of BP-M resulted in almost 75% reduction in cell viability which in case of other extracts was close to only 50% ( $P < 0.05$ ). These data were in line with PIP response as well, which showed a prominent dose-dependent inhibition of cell viability both at 24 h (Fig. 2d) and 48 h (Fig. 2h). Interestingly, the 48-h treatment of cells with PIP reduced the cell viability by ~80% with respect to vehicle-treated control cells (Fig. 2h) ( $P < 0.05$ ). Based on these data, it could be conceived that among the tested extracts, BP-M is most effective in preventing K-562 cell viability, which was just next to PIP in its potency. The cytotoxic effect of both BP-M (Fig. 2i) and PIP (Fig. 2j) was also tested on normal cell line, MRC-5 cell. As shown in Fig. 2i and j, there was no significant cell death in MRC-5 cells in response to either of them ( $P < 0.05$ ). We then determined the  $IC_{50}$  values of the test compounds in K-562 cell line. As shown in Table 4, BP-M was found to be most effective with an  $IC_{50}$  value of 193.6 and 116.6  $\mu$ g/ml at 24 and 48 h, respectively. The major metabolite of black pepper, i.e. PIP, which showed a prominent cytotoxic effect earlier, demonstrated an  $IC_{50}$  value of 148.2 and 56.3  $\mu$ M at 24 and 48 h, respectively. Based on these data among the tested extracts, only BP-M was selected for further analysis in the present study.

### Black pepper and piperine induce apoptosis leading to nuclear condensation in K-562 cells

The inhibitory effect of BP-M and PIP on K-562 cell proliferation was further ascertained by performing cell staining experiments followed by microscopic visualization. Firstly, the stage of early and late apoptosis was distinguished by uptake of AO/EB dye mixtures. For this experiment, the K-562 cells were treated with BP-M and PIP with concentrations equivalent to their respective  $IC_{50}$  values as obtained earlier. It has already been known that AO pervades both live and dead cells making the nucleus appear

**Table 2:** total phenolic and total flavonoid content in various black pepper extracts

Black pepper extract	Total phenolic content (GAE)	Total flavonoid content (QE)
BP-M	56.87 ± 2.01	92.14 ± 0.47
BP-E	57.64 ± 1.63	80.70 ± 1.45
BP-Aq	52.38 ± 1.99	98.81 ± 5.12

Data are the mean ± SEM of three independent experiments. BP-M, Black pepper methanol extract; BP-E, Black pepper ethanol extract; BP-Aq, Black pepper aqueous extract; GAE, µg gallic acid equivalent/g dry mass; QE, µg quercetin equivalent/g dry mass.

**Table 3:** GC-MS based metabolite profile of three different black pepper extracts

S. No.	Metabolites	NIST ID	Retention time (min)	Quantification ion	Relative metabolite content		
					BP-M	BP-E	BP-Aq
1	D-Limonene	79639	4.82	136, 121, 93, 68	89.55	131.23	3.51
2	Glycine	229287	7.296	147, 132, 114, 73	21.56	67.08	0.00
3	3-Methylcyclohexanol	229453	7.441	186, 171, 143, 73	1.69	3.53	3.70
4	Propanoic acid	290898	7.919	146,131, 75, 73	7.27	1604.97	447.17
5	Propanedioic acid	229341	8.147	321, 292, 147, 73	5.85	10.88	0.00
6	Terpinen-4-ol	109117	8.253	154, 136,111, 71	17.54	11.72	0.00
7	L-Valine	26146	8.72	261, 218, 144, 73	7.24	2.58	52.64
8	Acetic acid	227635	9.365	132, 117, 75, 73	1.98	2.62	2.48
9	4-Aminobutanoic acid	228101	9.871	247, 232, 147, 73	64.25	59.32	61.78
10	Butanedioic acid	229614	10.072	350, 335, 147, 73	159.70	145.74	167.69
11	α-Terpineol	114833	10.188	154, 136, 121, 59	13.37	7.31	0.00
12	Glyceric acid	150744	10.377	322, 292, 189, 73	138.77	155.09	32.70
13	Copaene	9240	10.572	204, 161, 119, 105	324.06	243.74	2.76
14	2-Methylglutaric acid	242292	10.694	275, 247, 147, 73	38.53	39.97	0.00
15	Serine	228085	10.778	321, 306, 204, 73	17.65	15.71	21.18
16	Phloroglucinol	118676	11.312	342, 327, 147, 73	74.73	56.36	55.74
17	Caryophyllene	291486	11.668	204, 189, 133, 93	2665.39	1866.06	899.99
18	cis-Carveol	107006	11.829	224, 209, 181, 73	126.82	152.18	112.87
19	β-Famesene	141000	11.896	204, 189, 133,69	229.78	212.9	234.19
20	Eugenol	291519	12.146	236, 221, 179, 73	65.40	43.09	12.41
21	Malic acid	228569	12.43	350, 335, 237, 73	153.99	102.83	77.00
22	β-Bisabolene	9654	12.658	204, 189, 161, 69	931.72	857.51	0.29
23	Erythritol	292004	12.747	410, 395, 217, 73	560.21	462.10	378.12
24	Catechol	78898	12.93	254, 239, 166, 73	19.15	28.15	10.34
25	Piperonylic acid	134278	13.025	265, 223, 179, 73	136.97	108.21	45.79
26	Pentanedioic acid	290975	13.425	318, 303, 204, 73	28.03	30.31	26.34
27	Asparagine	229288	13.759	348, 333,231, 73	34.64	30.48	19.40
28	D-Glucuronic acid	79257	14.365	539,305,204, 73	42.04	49.62	45.97
29	Arabinitol	79245	15.26	512, 307, 217, 73	279.82	19.04	4.65
30	Protocatechuic acid	162416	15.455	370, 355, 193, 73	291.88	186.81	113.83
31	Myristic acid	290632	15.694	299, 285, 117, 73	117.86	98.64	85.48
32	Fructose	228156	16.667	525, 437, 217, 73	217.57	233.08	140.21
33	D-Galactose	76356	16.729	540, 435, 204, 73	61.12	54.40	26.48
34	Syringic acid	291989	16.962	342, 327, 141, 73	110.12	87.00	51.76
35	Coumaric acid	6103	17.885	308, 293, 147, 73	1474.78	1268.75	110.80
36	Ferulic acid	234120	18.041	338, 323, 249, 73	22.92	27.74	4.95
37	Palmitic acid	151973	18.18	328, 313, 117, 73	248.79	163.84	5.28
38	Myo-inositol	7496	18.72	612, 305, 147, 73	114.43	226.90	3.79
39	Stearic acid	290961	19.448	356, 341, 117, 73	50.58	41.69	11.94
40	Pipecolic acid	436786	20.36	273, 230, 156, 73	53.62	55.26	36.92
41	Arachidic acid	379431	20.477	384, 369, 117, 73	6.85	9.46	6.41
42	Lignoceric acid	231005	21.156	440, 425, 117, 73	16.68	119.93	28.89
43	Piperine	152960	23.169	285, 201, 115, 84	3482.95	3015.11	143.47
44	Citric acid	228892	31.417	408, 393, 201, 73	79.65	91.11	38.23

BP-M, black pepper methanol extract; BP-E, black pepper ethanol extract; BP-Aq, black pepper aqueous extract; NIST, National Institute of Standards and Technology; metabolite content was expressed as µg phenyl phenol equivalent/g dry mass.

green, while EB permeates only those cells whose cytoplasmic integrity is compromised and approaching apoptosis or necrosis. As shown in Fig. 3a, the vehicle-treated group (control) had a

maximum number of viable cells (green) with regular cellular morphology and almost no penetration of EB. On the contrary, BP-M and PIP treated cells showed an increased count of EB stained

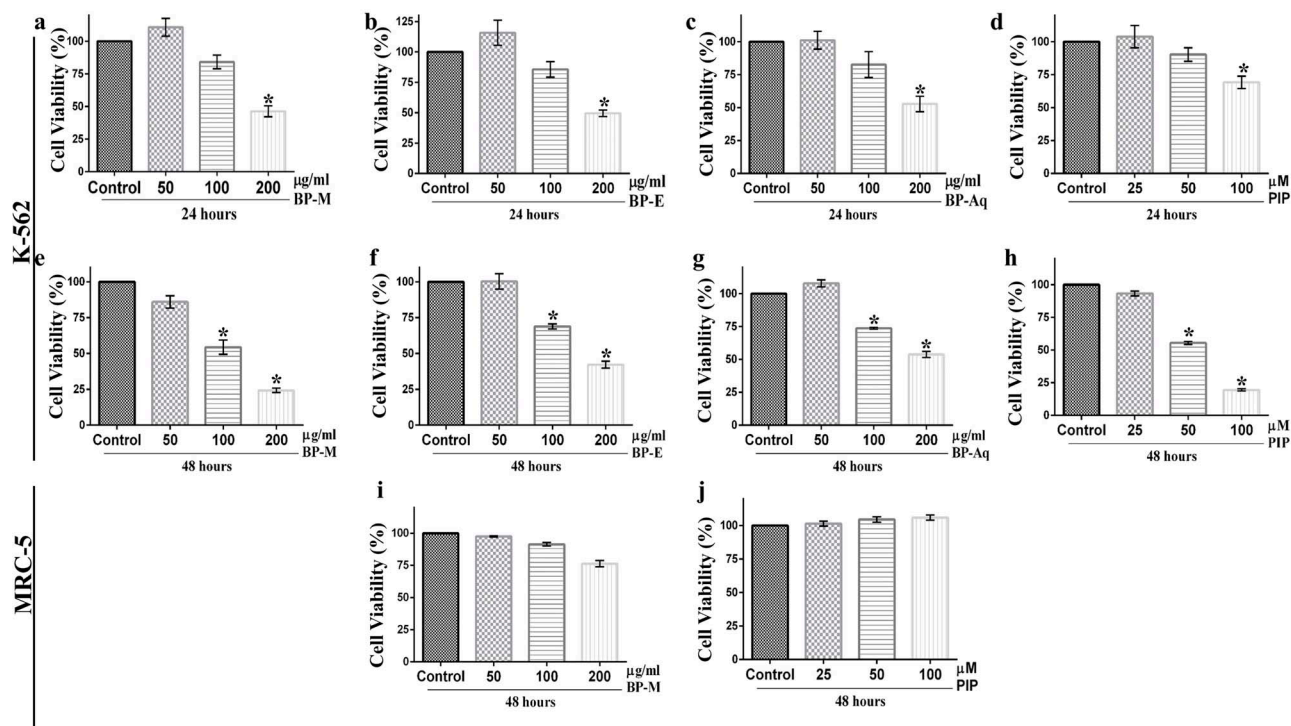


**Figure 2:** evaluation of the cytotoxic effect of black pepper extracts and piperine on K-562 cells. Viability of K-562 cells treated with black pepper extracts [methanol (a, e); ethanol (b, f) and aqueous (c, g)] and piperine (d, h) for varying periods of time, (a–d) 24 h and (e–h) 48 h, thereafter measured by MTT assay. The effect of (i) methanol extract and (j) piperine on the viability of MRC-5 cells after 48 h of treatment. All results are represented as mean  $\pm$  SEM of three independent experiments. \* indicates  $P < 0.05$  as compared with the respective vehicle-treated control group, which was considered as 100 percent in all cases. BP-M, black pepper methanol extract; BP-E, black pepper ethanol extract; BP-Aq, black pepper aqueous extract; PIP, piperine.

**Table 4:** inhibitory effects of various extracts of black pepper and its major constituent on the viability of K-562 cell line as determined by MTT assay

Extract type/phytochemical	Time period (hours)	IC <sub>25</sub> value (Mean $\pm$ SEM)	IC <sub>50</sub> value (Mean $\pm$ SEM)
BP-M	24	129.1 $\pm$ 7.6 $\mu$ g/ml	193.6 $\pm$ 8.3 $\mu$ g/ml
	48	66.6 $\pm$ 11.7 $\mu$ g/ml	116.6 $\pm$ 14.7 $\mu$ g/ml
BP-E	24	133.6 $\pm$ 6.5 $\mu$ g/ml	208.3 $\pm$ 3.5 $\mu$ g/ml
	48	83.33 $\pm$ 13.3 $\mu$ g/ml	153.8 $\pm$ 11.1 $\mu$ g/ml
BP-Aq	24	126.1 $\pm$ 8.9 $\mu$ g/ml	223.7 $\pm$ 3.5 $\mu$ g/ml
	48	109.6 $\pm$ 9.7 $\mu$ g/ml	201.3 $\pm$ 6.4 $\mu$ g/ml
PIP	24	93.8 $\pm$ 2.4 $\mu$ M	148.2 $\pm$ 6.2 $\mu$ M
	48	37.5 $\pm$ 3.4 $\mu$ M	56.3 $\pm$ 3.5 $\mu$ M

BP-M, black pepper methanol extract; BP-E, black pepper ethanol extract; BP-Aq, black pepper aqueous extract; PIP, piperine. Data are Mean  $\pm$  SEM of three independent experiments.

cells, confirming the cells to be in early apoptotic and/or late apoptotic stage. The loss of cytoplasmic membrane integrity and nuclear condensation was further confirmed by Hoechst 33258 dye staining. Hoechst dye visualizes changes in cellular nuclei and the formation of the apoptotic body through the appearance of intense blue coloration after binding to cellular DNA. As shown in Fig. 3b, BP-M and PIP caused intense nuclear condensation in K-562 cells when treated at respective IC<sub>50</sub> equivalent values of phytochemicals, while the vehicle-treated (control group) cells showed intact nuclear chromatin patterns.

Furthermore, the morphological changes in K-562 cells after 48 h treatment with BP-M and PIP were examined microscopically. As shown in Fig. 4a, the characteristics shrinkage and loss of confluent cell population were observed in both BP-M and PIP treated conditions, while cells in the vehicle-treated control group showed regular spherical cellular morphology. The rate of

cellular proliferation of K-562 cell lines was evaluated by trypan blue assay. The live-cell population of K-562 cells reduced by about 2- and 3-fold in response to IC<sub>50</sub> equivalent concentrations of BP-M and PIP, respectively, indicative of inhibition of proliferation and/or viability of K-562 cells ( $P < 0.05$ ) by these phytoconstituents (Fig. 4b).

### Black pepper and piperine induce intracellular ROS generation in K-562 cells to initiate cell death

It has already been reported that prior to undergoing apoptosis, generally, there is an augmentation of intracellular ROS levels in cells. Therefore, in our experiment, the intracellular ROS level was measured to determine the probable cause of apoptosis in cancer cells after treatment with BP-M and PIP at IC<sub>25</sub> and IC<sub>50</sub>

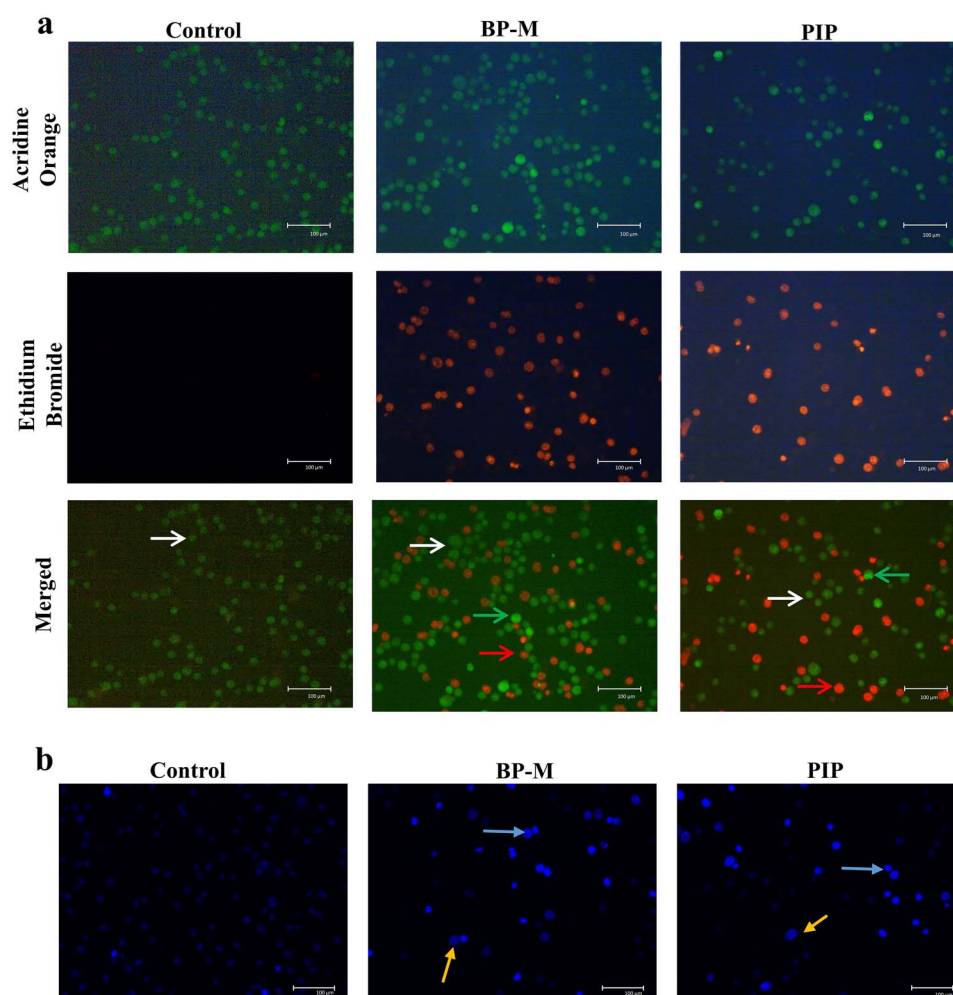


**Figure 3:** evaluation of apoptosis in response to black pepper. Representative (a) acridine orange/ethidium bromide dual staining and (b) Hoechst 33342 dye staining for nuclear condensation in apoptotic K-562 cells treated with methanol extract of black pepper and piperine at  $IC_{50}$  equivalent concentrations for 48 h. The images were visualized at  $200\times$  magnification using a fluorescent microscope. The experiment was performed three times independently. Arrows indicate (a) white, live cells, green, early apoptotic cells and red, late apoptotic cells; (b) blue, condensed chromatin; yellow, nuclear fragmentation. BP-M, black pepper methanol extract; PIP, piperine.

equivalent concentrations for 48 h. As shown in Fig. 5, when the phytochemicals (BP-M and PIP) and positive control ( $H_2O_2$ ) treated cells were analyzed through FACS after stained with DCFDA, the levels of accumulated ROS increased dramatically (purple color zone). The most pronounced effect was observed in response to  $IC_{50}$  concentrations for both BP-M and PIP, although both BP-M and PP showed significant ROS generation even at  $IC_{25}$  equivalent levels as well ( $P < 0.05$ ) (Fig. 5a). The results were further validated by quantifying the flow cytometry data where BP-M and PIP were found to increase the level of intracellular ROS in K-562 cells by 19.7- and 31.6-fold, respectively, in response to their respective  $IC_{50}$  equivalent concentrations ( $P < 0.05$ ) (Fig. 5b).

### Black pepper and piperine induce apoptosis in K-562 cells

In a milieu of cytotoxicity and microscopic observations, flow cytometry analysis was performed to examine the intensity with which the K-562 cells were undergoing apoptosis. The images as shown by FACS analysis divide the cell population into four quadrants with live cells in the lower left (LL) and dead cells in the upper left (UL). In contrast, the lower right (LR) and upper

right (UR) quadrant represent cells in early and late apoptosis, respectively. When K-562 cells were treated at  $IC_{25}$  and  $IC_{50}$  equivalent concentrations of BP-M and PIP for 48 h, apoptosis was distinctly observed as depicted by the distribution of cells in LR and UR quadrants. As shown in bar diagram of Fig. 6, the total apoptotic cells percentage (both early and late apoptotic cells) were found to be 67.17 and 79.58% (for BP-M) and 25.41 and 69.82% (for PIP) for individual phytochemical treated cells at  $IC_{25}$  and  $IC_{50}$  equivalent concentrations, respectively, as compared with vehicle-treated cells ( $P < 0.05$ ).

### Black pepper and piperine induce caspase-dependent apoptosis involving intrinsic pathway and downregulate PCNA expression

As it has already been reported that apoptosis is triggered by multi-signal pathways, transcriptional analysis of caspases and its activator genes was performed by semi-quantitative RT-PCR and quantitative RT-qPCR. In K-562 cells treated with  $IC_{25}$  and  $IC_{50}$  equivalent concentrations for 48 h, the expression of caspase-3 was found to increase by about 1.4- and 1.6-fold



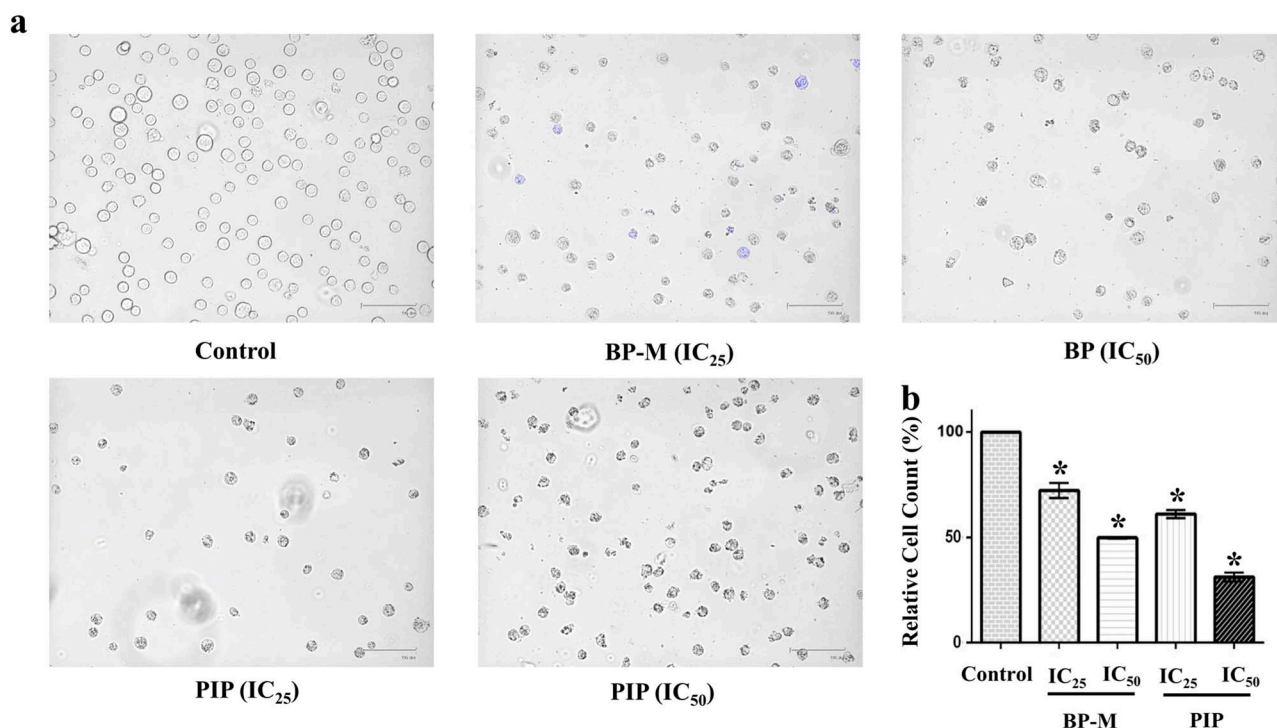


**Figure 4:** effect of black pepper methanol extract and piperine on the morphology and proliferation of K-562 cells. (a) Representative microscopic images of K-562 cells treated with respective phytochemicals at IC<sub>25</sub> and IC<sub>50</sub> equivalent concentrations for 48 h followed by trypan blue staining. (b) Bar graph representing the relative percentage count of K-562 cells as treated in (a) by trypan blue staining. Results are the mean  $\pm$  SEM of three independent experiments. \* represents  $P < 0.05$  as compared with the control group. BP-M, black pepper methanol extract; PIP, piperine; IC<sub>25</sub> and IC<sub>50</sub>, IC<sub>25</sub> and IC<sub>50</sub> equivalent concentrations, respectively.

in BP-M treated cells (Fig. 7a), while 1.7- and 1.9-fold in PIP-treated cells (Fig. 7b) at two dosages, respectively ( $P < 0.05$ ). In a similar pattern, the expression of caspase-9 increased by about 1.5- and 1.6-fold, respectively, in response to IC<sub>50</sub> equivalent concentrations of BP-M (Fig. 7a) and PIP (Fig. 7b) ( $P < 0.05$ ). The expression of apoptosis regulator gene, Bax, in treated cells were found to increase by about 1.4- and 1.6-fold in response to BP-M (Fig. 7a) and PIP (Fig. 7b), respectively, at their maximum concentrations. However, the level of Bcl-2 expression did not change under any treatment conditions (Fig. 7a and b). On the contrary, the level of transcription of PCNA was found to be downregulated by about 1.4- and 1.6-fold in BP-M (Fig. 7a) and PIP (Fig. 7b) treated cells, respectively, at IC<sub>50</sub> equivalent concentrations of both the phytochemicals ( $P < 0.05$ ). The expression patterns for caspase-9, caspase-3 and PCNA were also evaluated through quantitative RT-qPCR. A 2.2- and 1.5-fold increase in caspase-9 expression was observed in response to IC<sub>50</sub> equivalent concentrations of BP-M and PIP treatments, respectively (Fig. 7c) ( $P < 0.05$ ). In similar treatment conditions, the expression of caspase-3 was increased by 3.2- and 2.2-fold in response to IC<sub>50</sub> equivalent concentrations of BP-M and PIP, respectively (Fig. 7c) ( $P < 0.05$ ). As expected, the expression of PCNA was downregulated by 6.7- and 1.6-fold in the presence of IC<sub>50</sub> equivalent concentrations of BP-M and PIP, respectively (Fig. 7c) ( $P < 0.05$ ).

To assess if the impact of test phytochemicals is linked to both, transcription as well as translation of target genes, in the next phase, we determined changes in the level of proteins of the same genes as discussed above by immunoblot analysis. For this experiment, K-562 cells were treated similarly at IC<sub>25</sub> and IC<sub>50</sub> equivalent concentrations of both BP-M and PIP for 48 h. As shown in Fig. 8, the expression of cleaved caspase-3 was

found to be upregulated by about 6.1- and 7.6-fold, respectively, in response to IC<sub>50</sub> equivalent concentration of BP-M (Fig. 8a) and PIP (Fig. 8b) ( $P < 0.05$ ). The expression of caspase-9 and Bax was also found to be upregulated by about 3.5- and 6.5-fold, respectively, in response to IC<sub>50</sub> equivalent concentration of BP-M (Fig. 8a) ( $P < 0.05$ ). A similar trend of upregulation was also observed in response to PIP for caspase-9 and Bax (2.1- and 3.7-fold, respectively) at IC<sub>50</sub> equivalent concentrations (Fig. 8b) ( $P < 0.05$ ). Interestingly, in accordance to our transcription data (Fig. 7a and b), the level of translation of Bcl-2 also did not show any significant change in response to PIP (Fig. 8b) with respect to the vehicle-treated groups ( $P < 0.05$ ), whereas a 2-fold reduction was observed in the presence of BP-M (Fig. 8a). This aspect of differential transcription and translation patterns for Bcl-2 in response to BP-M needs further validation involving detailed studies. When tested for PCNA, the expression profile showed a decrease by about 2.7- and 1.5-fold in response to BP-M (Fig. 8a) and PIP (Fig. 8b), respectively, in response to IC<sub>50</sub> equivalent concentrations of phytochemicals with respect to vehicle-treated cells ( $P < 0.05$ ). Thus, taken together, it can be speculated that both BP-M and PIP induce the intrinsic pathway of apoptosis in K-562 cells while regulating its proliferation and inducing cytotoxicity.

#### **In silico investigation of piperine confirms the activation of Apaf-1 and inhibition of Bcl-2 and PCNA**

The binding patterns of PIP with possible target proteins (Bcl-2, PCNA and Apaf-1) were investigated using computational-based docking studies. Following our earlier experimental data where we showed the regulation of most of the (anti)apoptotic genes by BP-M and PIP, our docking study also substantiated the same

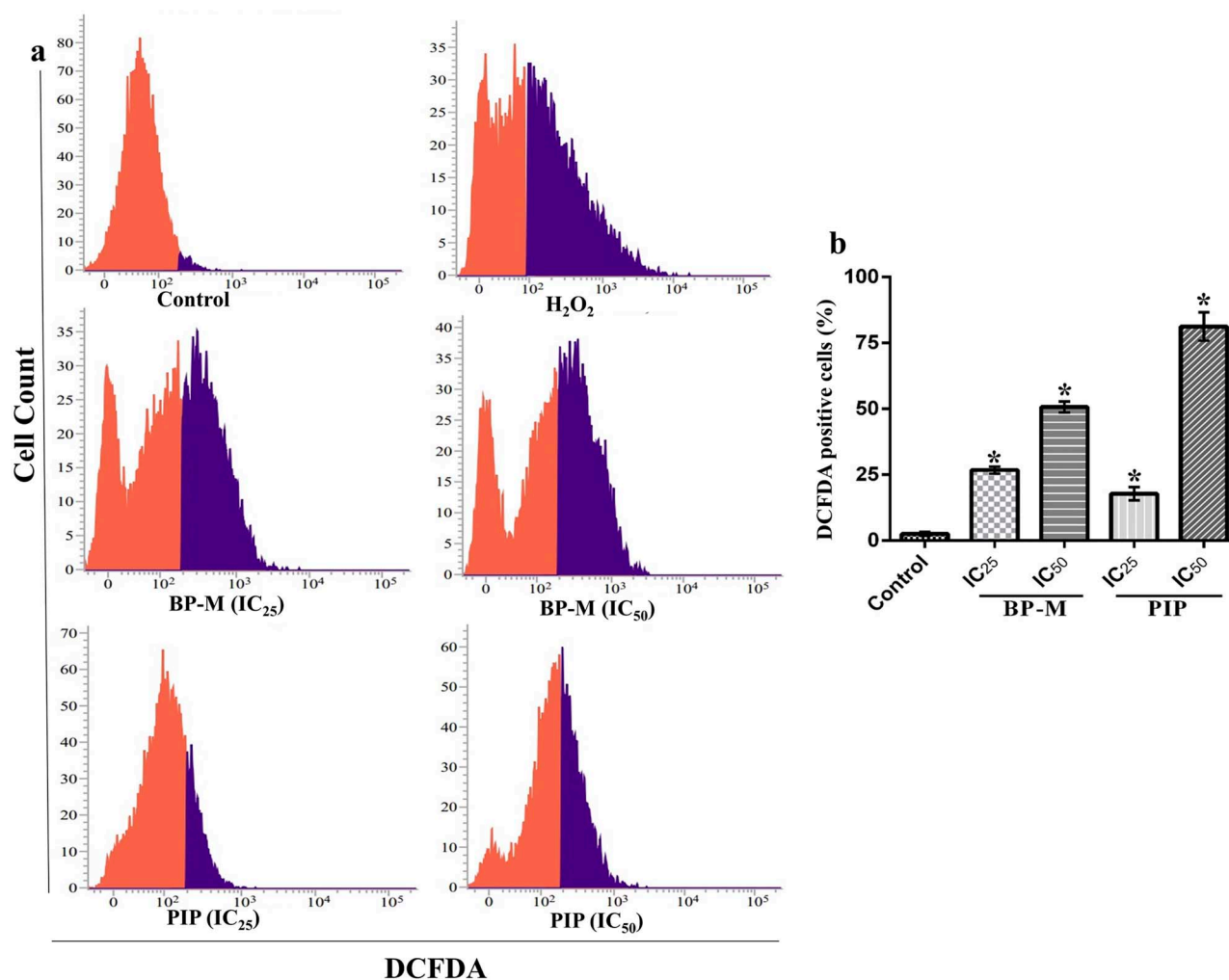


**Figure 5:** treatment of black pepper methanol extract and piperine (IC<sub>25</sub> and IC<sub>50</sub>, 48 h) induces the generation of ROS in K-562 cells. (a) Representative FACS analysis of cells using DCFDA staining. Red and purple zone represents unstained and stained cells, respectively. (b) Bar graph indicating the percentage of DCFDA stained K-562 cell count determined by FACS analysis as treated in (a). Results are the representation of three independent experiments with mean  $\pm$  SEM. \* indicates  $P < 0.05$  as compared with control group. BP-M, black pepper methanol extract; PIP, piperine; IC<sub>25</sub> and IC<sub>50</sub>, IC<sub>25</sub> and IC<sub>50</sub> equivalent concentrations, respectively.

where PIP showed binding with all these proteins. The predicted binding energy and affinity of PIP against these three proteins are presented in Table 5.

PIP was involved in binding with Apaf-1 through polar as well as with non-polar interactions (Fig. 9), and the binding site of PIP was found to be the same as in the complex structure of Apaf-1 with its activator ADP. Binding energy and binding constants were calculated using Autodock scoring function, and they were found to be  $-8.65$  kcal/mol and  $0.456$   $\mu$ M, respectively. The overall structure of Apaf-1 with docked PIP in the active site, and deep buried active site are shown in Fig. 9a and b, respectively. PIP was found to interact with SER325, GLY159 and LYS160 residues of Apaf-1 using hydrogen bond mediated binding (Fig. 9c and d), while CYS158, MET155, PRO123, SER325, VAL125, LEU322, SER161, HIS438, GLY157, LYS160, GLY159 and PRO321 residues of Apaf-1 interacted with PIP through hydrophobic interactions (Fig. 9c and d).

When we analyzed the interaction of PIP with the next protein target, i.e. PCNA, it showed that both hydrophobic as well as hydrophilic interactions play a significant role in the binding of

PIP with PCNA (Fig. 10). The binding energy and binding constant of PIP with PCNA were found to be  $-7.53$  kcal/mol and  $3.03$   $\mu$ M, respectively (Table 5). The PIP bound docked PCNA structure is shown in Fig. 10a and surface diagram indicating the deep cavity that interacts with PIP- box (PCNA interacting protein box) is shown in Fig. 10b. The binding patterns showed that GLU25 and LEU126 residues of PCNA were involved in the binding with PIP through hydrogen bonding (Fig. 10c and d). Other residues that seemed to be involved in the binding through hydrophobic interactions were ASP29, CYS27, GLU25, ASN24, ILE23, SER42, ASP41, HIS44, MET40, GLU124, LEU126, GLN38 and VAL123 (Fig. 10c and d and Table 5).

Like that of Apaf-1 and PCNA, PIP was also found to interact and bind to Bcl-2 through both hydrophobic and hydrophilic interactions. Figure 11 shows the different aspects of PIP binding with Bcl-2. The overall structure of Bcl-2 with docked PIP is shown in Fig. 11a. The active site pocket of Bcl-2 with docked PIP is shown in the surface diagram (Fig. 11b). Based upon the analysis of best docked pose, it has been found that ARG105 interacted with PIP through hydrogen bonding (Fig. 11c and d),

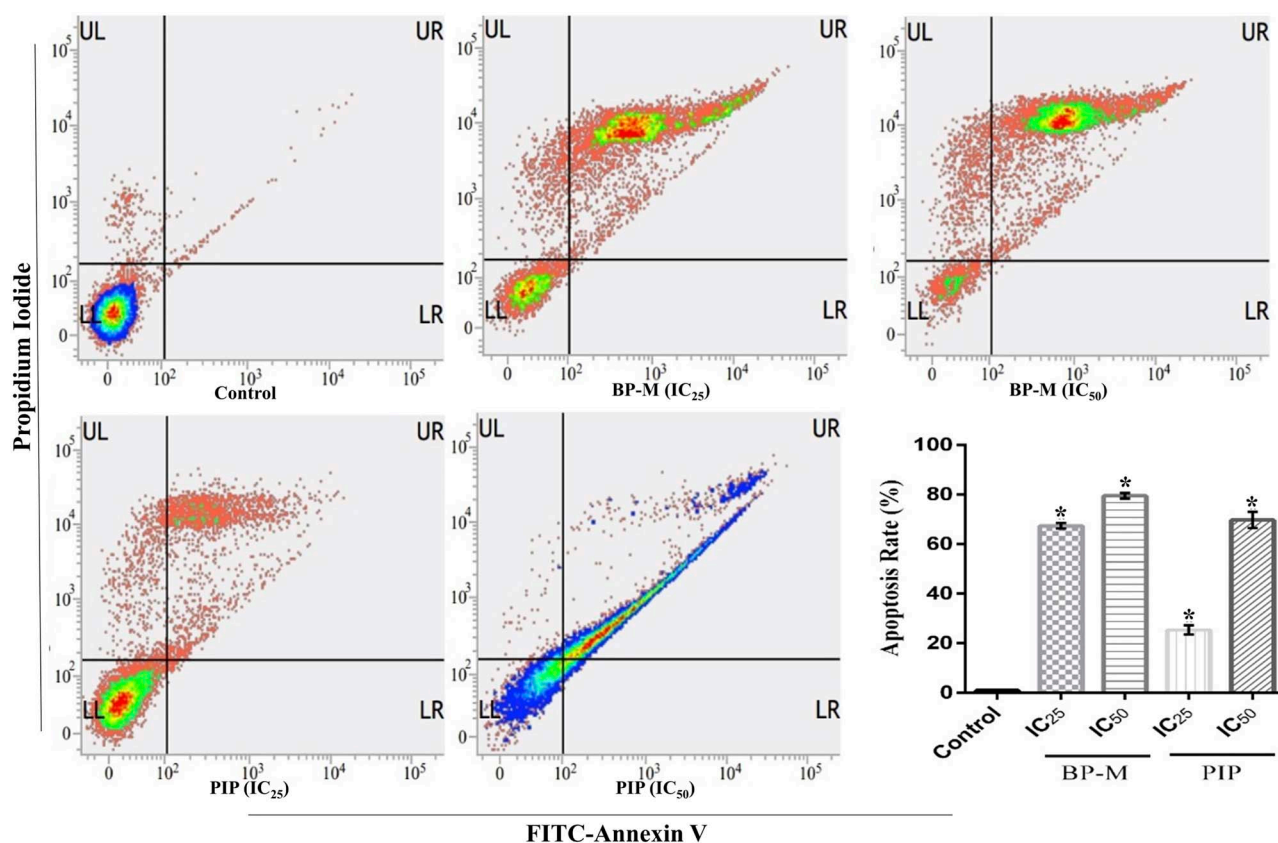


**Figure 6:** effect of black pepper methanol extract and piperine (IC<sub>25</sub> and IC<sub>50</sub>, 48 h) on apoptosis in K-562 cells. Representative FACS analysis of the cells performed using Annexin V as a marker. Bar graph indicating the sum of cells in the UR and LR quadrants of respective treatment groups. Each bar indicates mean  $\pm$  SEM of three independent experiments and expressed as percent apoptosis rate. \* represents  $P < 0.05$  as compared with the control group. UL, upper left; UR, upper right; LL, lower left; LR, lower right; BP-M, black pepper methanol extract; PIP, piperine; IC<sub>25</sub> and IC<sub>50</sub>, IC<sub>25</sub> and IC<sub>50</sub> equivalent concentrations, respectively.

**Table 5:** predicted binding parameters and interactions of piperine with respective protein targets

Target protein	Binding constant ( $\mu\text{M}$ )	Binding energy (kcal/mol)	Residues involved in binding	Residues involved in H-bonding
Apaf-1	0.456	-8.65	ASP244, SER161, HIS438, PRO123, VAL125, SER325, LEU322, PRO321, GLY159, GLY157, CYS158, LYS160, MET155, ARG265	SER325, GLY159, LYS160
PCNA	3.03	-7.53	ASP29, CYS27, GLU25, ASN24, ILE23, SER42, ASP41, HIS44, MET40, GLU124, LEU126, GLN38, VAL123	GLU25, LEU126
Bcl-2	41.14	-5.98	TYR67, ARG66, PHE63, ASP62, ALA59, ALA108, LEU96, ARG105, GLY104, ASN102	ARG105

while residues that contributed to binding through hydrophobic interactions were found to be LEU96, ALA108, GLY104, ARG66, ASP62, PHE63 and ARG105 (Fig. 11c and d).

## Discussion

It is since ancient times that black pepper has been used popularly in culinary practices across the globe. Black pepper, along with its major bioactive component, i.e. PIP, has been evaluated for its medicinal properties widely. Black pepper improves the functioning of the digestive system and also imparts antioxidant, antidiarrheal, antidepressant, anti-inflammatory, anti-diabetic and anti-tumor activity along with various other healthcare benefits [29]. *In vitro* investigation has confirmed the role of

black pepper and PIP in the inhibition of proliferation of colon cancer cells [12] and androgen-dependent and independent prostate cancer cells [11]. According to some recent reports, black pepper has also been shown to improve breast cancer [10] and lung adenocarcinoma [13] conditions, while Brazilian *Piper* species has been found to be cytotoxic towards oral carcinoma cells [30].

In the present study, all three black pepper extracts (methanol, ethanol and aqueous) were found to be a rich source of phenolic and flavonoid compounds, which suggested for its pharmacological potential. GC-MS analysis confirmed that PIP is the major metabolite present in black pepper extract. The other metabolites present in the black pepper extract in considerable amounts were caryophyllene, a terpenoid with

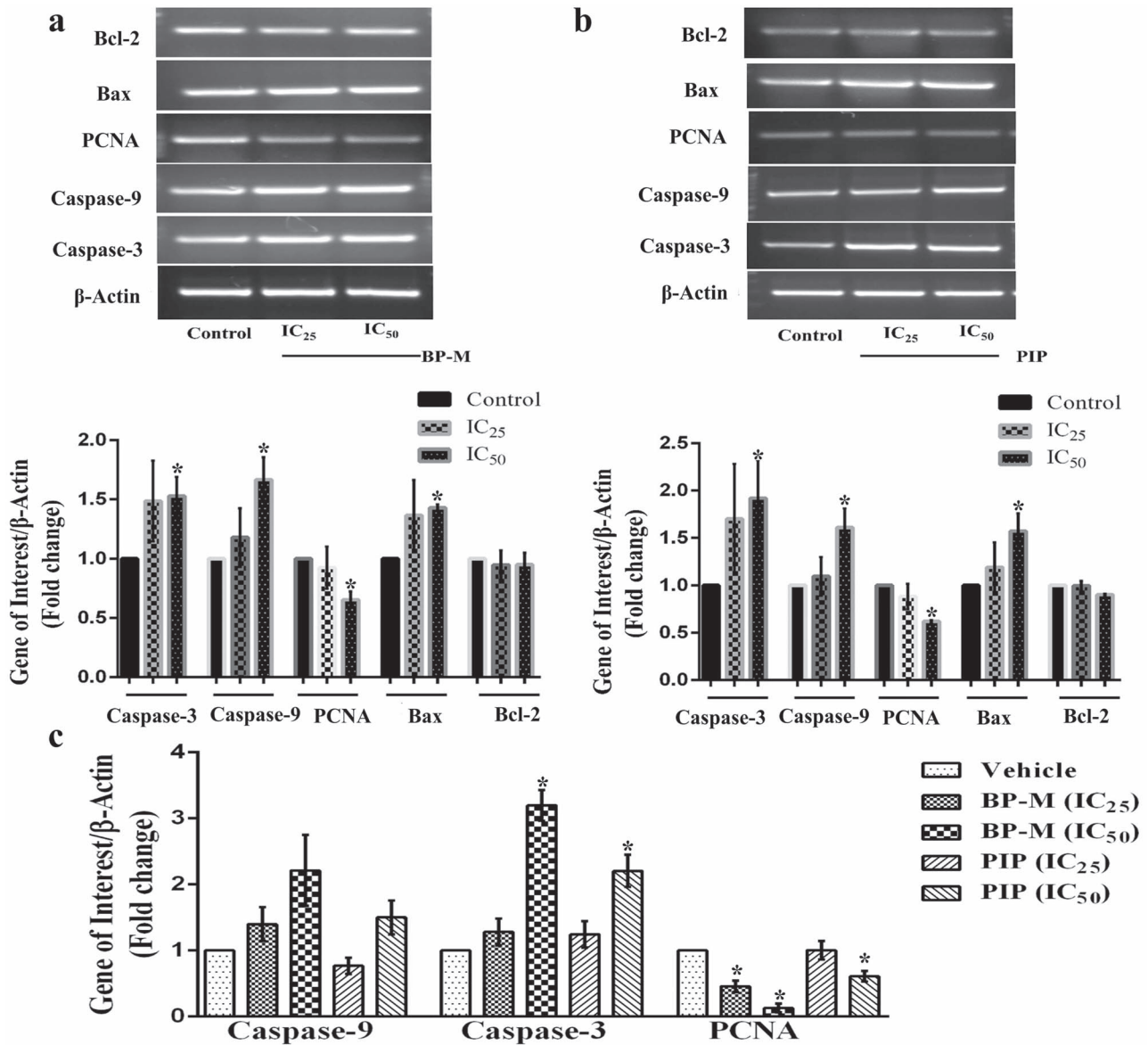


**Figure 7:** effect of black pepper methanol extract and piperine (IC<sub>25</sub> and IC<sub>50</sub>, 48 h) in regulating the transcription of some (anti)apoptotic genes in K-562 cells. Representative semi quantitative PCR images indicating the transcriptional patterns of various caspase, pro- and anti-apoptotic genes in response to (a) black pepper methanol extract and (b) piperine.  $\beta$ -actin was used as a gel loading control. Bar graph below respective gel images represent fold change in expression as compared to the respective vehicle-treated control group. (c) The relative quantification of mRNA expression of caspase-9, caspase-3 and PCNA genes using RT-qPCR in K-562 cells after treatment with black pepper methanol extract and piperine. Results are the mean  $\pm$  SEM of three independent experiments. \* indicates  $P < 0.05$  as compared with the respective control groups for each genes. BP-M, black pepper methanol extract; PIP, piperine; IC<sub>25</sub> and IC<sub>50</sub>, IC<sub>25</sub> and IC<sub>50</sub> equivalent concentrations, respectively, at 48 h.

anticancer property [31] and *P*-coumaric acid, a phenolic acid which has cytotoxic activity against various tumor conditions and also has been reported to show antioxidant, antimicrobial and antiviral properties [32]. PIP has been widely studied for its potent role in different cancer conditions, bio-enhancement of various other drugs and prevention of various chronic disease conditions [33]. Based on these facts, PIP is considered as one of the most bioactive metabolites of the pepper family. Altogether, these studies and phytochemical investigations led us to analyse the anticancer potential of black pepper and its major constituent PIP against unexplored CML conditions. Initial cellular proliferation studies showed the potential of both black pepper extracts and PIP to be effective cytotoxic

phytochemicals against CML. Among three extracts tested by us, the methanol extract was found to be most potent one. This could be attributed to comparatively high proportion of PIP in this extract as compared with other two extracts. At the same time, methanol extract was also found to be marginally more effective than PIP alone, atleast in some of the parameters as tested by us. This actually indicates a pattern of combined effect by various phytoconstituents present in the extract which at times may be more than the isolated compounds, as claimed by various traditional healthcare systems. However, all these aspects need further detailed studies in order to establish the concentration dependent effects of various metabolites in black pepper.

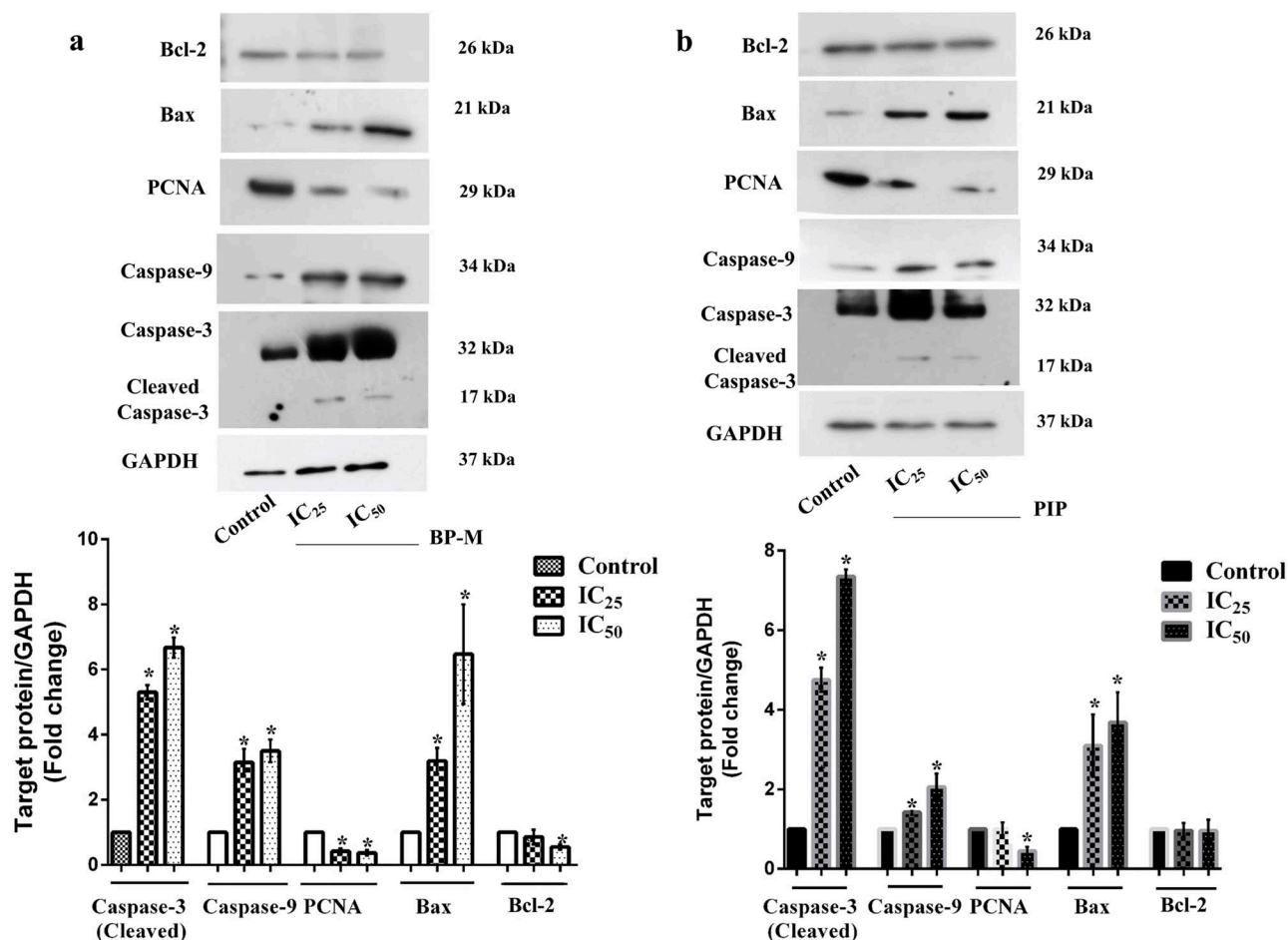


**Figure 8:** effect of black pepper methanol extract and piperine (IC<sub>25</sub> and IC<sub>50</sub>, 48 h) in regulating the translation of (anti)apoptotic genes in K-562 cells. Representative protein expression patterns of various caspase, pro- and anti-apoptotic genes as determined by immunoblot analysis in response to (a) black pepper methanol extract and (b) piperine. GAPDH was used as a gel loading control for immunoblot analysis. Bar graph below respective gel images represent fold change in expression as compared with the respective vehicle-treated control group. Results are the mean  $\pm$  SEM of three independent experiments. \* indicates  $P < 0.05$  as compared with the respective control group in each protein. BP-M, black pepper methanol extract; PIP, piperine; IC<sub>25</sub> and IC<sub>50</sub>, IC<sub>25</sub> and IC<sub>50</sub> equivalent concentration, respectively, at 48 h.

The calcium-dependent phospholipid flip flop movement along with the loss of aminophospholipid translocase activity leads to the appearance of phosphatidylserine in outer leaflets of the plasma membrane of apoptotic cells. Annexin V selectively binds with the exposed phosphatidylserine protein moiety and distinguishes the apoptotic cells from non-apoptotic ones [34]. Earlier, it has been reported that PIP induces late apoptosis in triple-negative breast cancer cells [35]. In our study, the flow cytometry analysis by Annexin V assay elucidated a dose-dependent increase in Annexin V positive cells in the presence of both black pepper and PIP, confirming the occurrence of apoptotic cell death. These results are in accordance with the progression of cancer prevention conditions, as confirmed earlier [35].

Cysteinylnaspartateprotease (caspase) enzymes family is the executioner of programmed cell death called apoptosis. The progression of apoptosis is regulated by two distinctively interconnected pathways, namely extrinsic and intrinsic pathways. Caspase-8 and -9 are two initiator caspases which exist as inactive procaspase monomers. Caspase-8 leads to the extrinsic pathway involving various death receptors such as tumor necrosis factor receptor 1, Apo-1, Apo-2, Apo-3 and nerve growth

factor receptor [36]. Caspase-9 initiates mitochondria-assisted intrinsic pathway involving the Bcl-2 protein family. Bcl-2 proteins family involves different pro- and anti-apoptotic proteins. The generation of stress signals within cell inhibits the anti-apoptotic proteins (Bcl-2, Bcl-xL) and promotes the assembly of pro-apoptotic protein (Bak-Bax) oligomers within the outer mitochondrial membrane and thus leading to the formation of apoptosomes. The activation of pro-initiator caspases further activates executioner caspases (-3, -6 and -7) [37]. PIP has a structural similarity with piperidine, which also has been reported to have anticancer properties. Piperidine and its various structural analogs have been reported to demonstrate cytotoxic effects against K-562 cells [38] and gliomas [39]. PIP has been reported to induce caspase activation leading to the inhibition of human colon cancer growth [12, 40]. In the current study, the situation of apoptosis in K-562 cells was found to be associated with an increase in the level of Bax protein, which leads to its hetero-dimerization with Bcl-2 protein and inhibiting its expression. In our study, surprisingly, the transcription of Bcl-2 was not altered either by BP-M or PIP, although the latter was able to inhibit the translation of this protein and

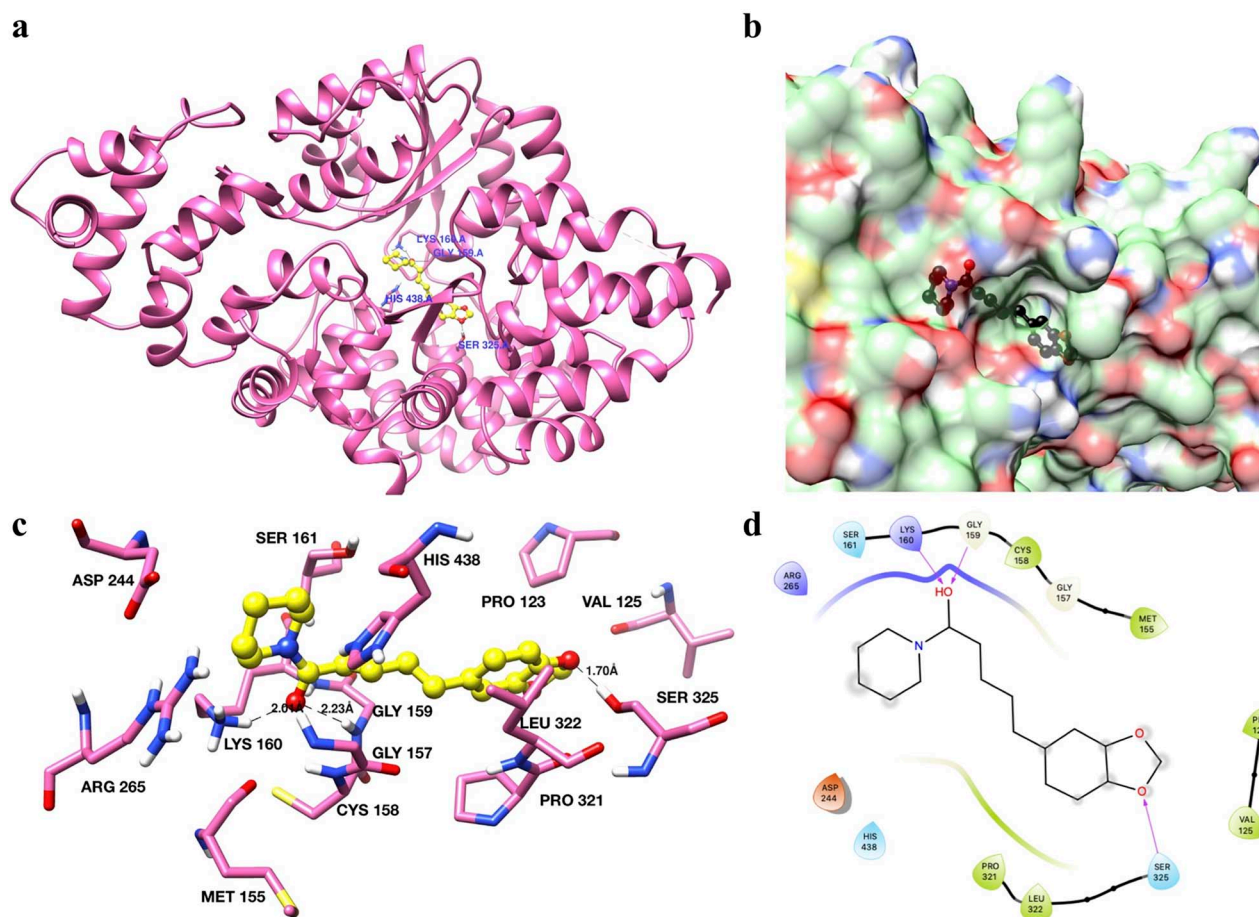


**Figure 9:** binding analysis of piperine with Apaf-1. (a) The overall structure of Apaf-1 (ribbon diagram) with piperine docked in the active site shown in yellow color and ball and stick representation. Interacting residues are shown in sticks and labeled blue. (b) Surface diagram of Apaf-1 protein showing the binding pockets. Piperine is shown in black color. (c) Interactions of piperine with the active site residues of Apaf-1. Interacting residues are shown as sticks and in hot pink color. Piperine is shown in yellow color with a ball and stick representation. Hydrogen bonds are labeled and shown as black dash lines. (d) 2D interaction diagram of piperine with Apaf-1.

also showed prominent binding to Bcl-2 protein in docking studies. This aspect needs further detailed validation in future studies. This increased ratio of Bax/Bcl-2 in cells lead to the release of cytochrome c in the cytosol from its mitochondrial compartments, which bind to the Apaf-1 factor of cells and activates caspase-9 [18, 41].

Every aerobic cell maintains various biochemical antioxidants and ROS in its milieu. The generation of oxidative stress leads to an imbalance between ROS and antioxidant moieties. It has been already reported that various therapeutic agents generate oxidative stress and are selectively toxic to tumors [42, 43]. The generation of ROS leads to the activation of pro-apoptotic protein such as Bax and another pathway such as the MAPK pathway, which trigger changes in mitochondrial membrane permeability, subsequently leading to mitochondria-dependent cell death pathway. In the present study, both black pepper and PIP generated ROS in K-562 cells and also increased the Bax/Bcl-2 ratio, which might have led to the release of cytochrome C from mitochondria. This in turn leads to the formation of apoptosomes with Apaf-1, thus initiating intrinsic pathway and finally causing the activation of caspase-9/-3 cascade [44, 45]. However, the level of caspase-8 remained unchanged in response to both black pepper and PIP (data not shown).

PCNA is a non-histone, cell nuclear protein that performs the crucial cell survival functions by regulating DNA replication and DNA repair mechanisms. The regulation of PCNA is considered as a hallmark of proliferating cells. The activation of executioner caspase-3 leads to the degradation of PCNA interacting peptides into short PCNA binding peptides. These peptides functionally inactivate PCNA, making it unavailable for functioning [46]. The expression of PCNA has been shown to be downregulated both in the presence of black pepper and PIP at transcription as well as translational level, which may be considered as the final impetus for cells to enter apoptosis.

Molecular docking is considered as an indispensable computational tool in structural biology and drug design studies [47]. In the current study, the preliminary *in silico* analysis supported *in vitro* data obtained earlier. The macromolecule–ligand interaction study by molecular docking showed that PIP interacts through hydrophobic and hydrophilic interactions, which might be responsible for the inhibition of Bcl-2 and PCNA. By comparing the predicted binding pose of PIP docked PIP-Bcl-2 complex with the N-heteroaryl sulfonamide-bound Bcl-2 (PDB ID:4IEH), it was found that PIP binds with Bcl-2 in a similar fashion interacting with the key residues (TYR67, ARG66, ASP62 and ALA59).

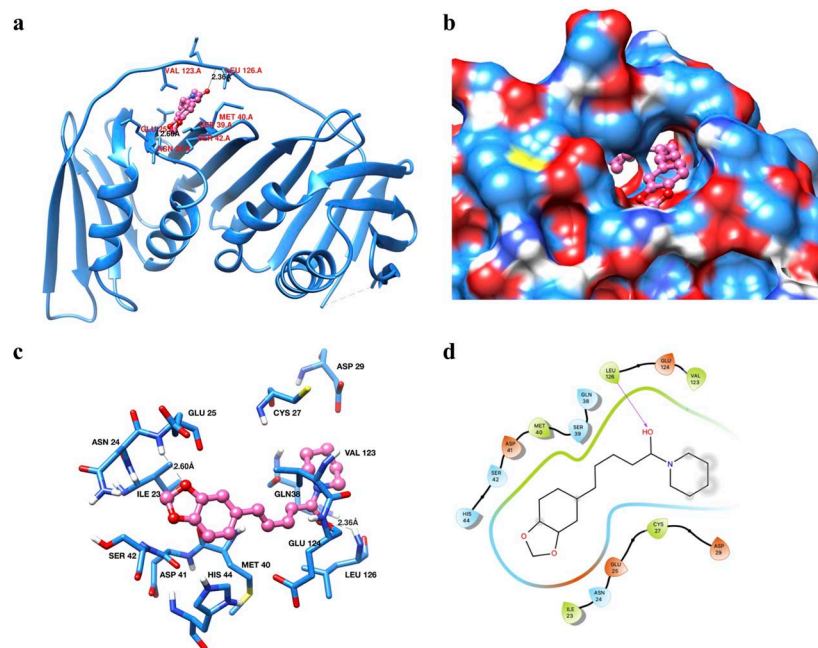


**Figure 10:** binding analysis of piperine with PCNA. (a) Ribbon diagram of PCNA protein showing the different secondary structure elements and PIP in the binding site pocket (shown in hot pink color and ball and stick representation). Interacting residues are shown in dodger blue color as sticks. (b) Surface diagram of PCNA showing the active site pocket with piperine (hot pink color and ball-stick representation). (c) Interactions of piperine with the active site residues of PCNA. Interacting residues are in dodger blue color and shown in sticks representation. Piperine is shown in hot pink color as a ball and stick. Hydrogen bonds are labeled and shown as black dashed lines. (d) 2D interaction diagram of piperine with PCNA.

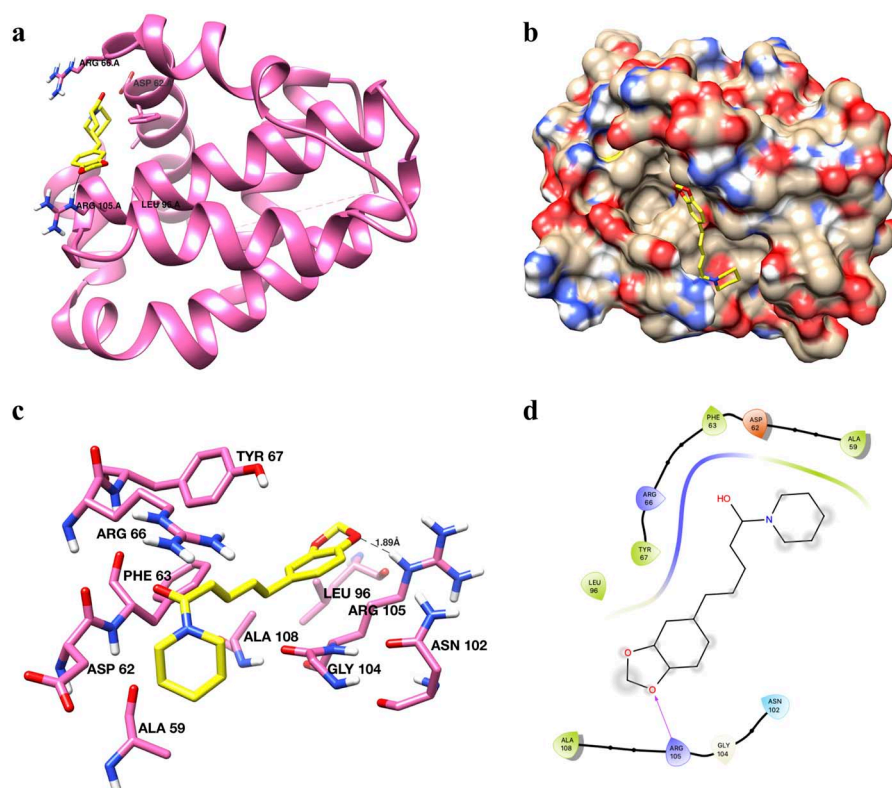


**Figure 11:** binding of piperine with Bcl-2. (a) Ribbon diagram of Bcl-2 with piperine in the active site. Piperine has been shown in yellow color and stick representation. Interacting residues are shown in hot pink color as sticks. (b) Surface diagram of Bcl-2 protein with piperine (yellow color and stick representation) showing the active site pocket. (c) Interaction of piperine with the critical residues of Bcl-2. Interacting residues are shown in hot pink color as sticks. Piperine is shown in yellow color as sticks. Hydrogen bonds are labeled and shown as black dash lines. (d) 2D interaction diagram of piperine with Bcl-2.

Similarly, PIP-PCNA docked conformation compared with the ligand-bound crystal structure of PCNA (PDB ID: 3WGW) confirmed the binding of PIP with the PIP-box cavity of PCNA, which might be responsible for its inhibition [26]. Apaf-1 is an essential protein that leads to the formation of apoptosomes, which in turn, leads to the activation of caspase-9. The active conformation of Apaf-1 confirms ATP/ADP hydrolysis [27]. The strong binding of PIP to the ADP binding site of Apaf-1, as observed in molecular docking analysis, confirmed that it might also lead to Apaf-1 activation, which ultimately causes the activation of caspase-9 and the initiation of the intrinsic apoptotic pathway to prevent the proliferation of cancerous cells. Altogether, these observations indicate that both black pepper and PIP has the potentiality to prevent the progression of CML.

In conclusion, the findings reported in this study preliminarily affirm that both black pepper and its main metabolite PIP are potent impediment of cellular proliferation in leukemic cells. These phytochemicals initiate the persuasion of apoptosis in human CML cells by upregulating genes involved in intrinsic pathway, i.e. caspase-9, -3 and Bax and subsequent downregulation of PCNA expressions. The cytotoxic potential of both black pepper and PIP increases with the progression of time and dose of treatments. Based on these data, it could be accepted that the involvement of black pepper in regular dietary practice may prevent the development of CML. Therefore, further in detailed studies involving more precise and specific *in vitro* and *in vivo* experimental models are warranted to appreciate the highly effective therapeutic potential of black pepper and its major metabolite, i.e. PIP, for which these data sets as reported in this study would provide a strong supportive base.

## Supplementary data

Supplementary data is available at TOXRES Journal online.

## Funding

This work was supported by a research fellowship (JRF/SRF) assisted in pursuing doctoral research to S.B. and P.K. (CSIR, India).

## Conflict of interest statement

The authors declare that they have no conflicts of interest.

## Authors' contribution

S.B. and P.R. designed the study. S.B. completed the experiment process, literature search and generation of figures. S.B. and P.R. wrote the manuscript, while P.K., V.K., S.S.S., R.V., V.D.K. and D.S. edited the manuscript. All authors read and approved the final manuscript.

## Consent for publication

Not applicable.

## Ethics approval and consent to participate

Not applicable.

## References

- Eaton L. World cancer rates set to double by 2020. *BMJ* 2003;**326**:728. doi: [10.1136/bmj.326.7392.728/a](https://doi.org/10.1136/bmj.326.7392.728/a).
- IHME (2020). Global burden of diseases. *Lancet*. <https://www.thelancet.com/lancet/visualisations/gbd-compare> (4 January 2020, date last accessed).
- Ureshino H, Shindo T, Kimura S. Role of cancer immunology in chronic myelogenous leukemia. *Leuk Res* 2020;**88**:106273. doi: [10.1016/j.leukres.2019.106273](https://doi.org/10.1016/j.leukres.2019.106273).
- Jabbour E, Kantarjian H. Chronic myeloid leukemia: 2020 update on diagnosis, therapy and monitoring. *Am J Hematol* 2020;**95**:691–709. doi: [10.1002/ajh.25792](https://doi.org/10.1002/ajh.25792).
- Massimino M, Stella S, Tirrò E et al. ABL1-directed inhibitors for CML: efficacy, resistance and future perspectives. *Anti-cancer Res* 2020;**40**:2457–65. doi: [10.21873/anticancerres.14215](https://doi.org/10.21873/anticancerres.14215).
- Deininger M, O'Brien SG, Guilhot F et al. International randomized study of interferon Vs STI571 (IRIS) 8-year follow up: sustained survival and low risk for progression or events in patients with newly diagnosed chronic myeloid leukemia in chronic phase (CML-CP) treated with Imatinib. *Blood* 2009;**114**:1126. doi: [10.1182/blood.V114.22.1126.1126](https://doi.org/10.1182/blood.V114.22.1126.1126).
- Ramawat KG, Goyal S. The Indian herbal drugs scenario in global perspectives. In: Ramawat KG, Merillon JM (eds). *Bioactive Molecules and Medicinal Plants*. Berlin, Heidelberg: Springer Berlin Heidelberg, 2008, 325–47. doi: [10.1007/978-3-540-74603-4\\_18](https://doi.org/10.1007/978-3-540-74603-4_18).
- Ahmad N, Fazal H, Abbasi BH et al. Biological role of *Piper nigrum* L. (black pepper): a review. *Asian Pac J Trop Biomed* 2012;**2**:S1945–53. doi: [10.1016/S2221-1691\(12\)60524-3](https://doi.org/10.1016/S2221-1691(12)60524-3).
- Smilkov K, Ackova DG, Cvetkovski A et al. Piperine: old spice and new nutraceutical? *Curr Pharm Des* 2019;**25**:1729–39. doi: [10.2174/1381612825666190701150803](https://doi.org/10.2174/1381612825666190701150803).
- Deng Y, Sriwiriyan S, Tedasen A et al. Anti-cancer effects of *Piper nigrum* via inducing multiple molecular signaling *in vivo* and *in vitro*. *J Ethnopharmacol* 2016;**188**:87–95. doi: [10.1016/j.jep.2016.04.047](https://doi.org/10.1016/j.jep.2016.04.047).
- Ouyang D, Zeng L, Pan H et al. Piperine inhibits the proliferation of human prostate cancer cells via induction of cell cycle arrest and autophagy. *Food Chem Toxicol* 2013;**60**:424–30. doi: [10.1016/j.fct.2013.08.007](https://doi.org/10.1016/j.fct.2013.08.007).
- Yaffe PB, Power Coombs MR, Doucette CD et al. Piperine, an alkaloid from black pepper, inhibits growth of human colon cancer cells via G1 arrest and apoptosis triggered by endoplasmic reticulum stress. *Mol Carcinog* 2015;**54**:1070–85. doi: [10.1002/mc.22176](https://doi.org/10.1002/mc.22176).
- Marques da Fonseca L, Jacques da Silva LR, Santos dos Reis J et al. Piperine inhibits TGF- $\beta$  Signaling pathways and disrupts EMT-related events in human lung adenocarcinoma cells. *Medicines* 2020;**7**:19. doi: [10.3390/medicines7040019](https://doi.org/10.3390/medicines7040019).
- Lang SJ, Schmiech M, Hafner S et al. Antitumor activity of an *Artemisia annua* herbal preparation and identification of active ingredients. *Phytomedicine* 2019;**62**:152962. doi: [10.1016/j.phymed.2019.152962](https://doi.org/10.1016/j.phymed.2019.152962).
- Srivastava JK, Gupta S. Antiproliferative and apoptotic effects of chamomile extract in various human cancer cells. *J Agric Food Chem* 2007;**55**:9470–8. doi: [10.1021/jf071953k](https://doi.org/10.1021/jf071953k).
- Sarkate A, Banerjee S, Mir JI et al. Antioxidant and cytotoxic activity of bioactive phenolic metabolites isolated from the yeast-extract treated cell culture of apple. *Plant Cell Tiss Org Cult* 2017;**130**:641–9. doi: [10.1007/s11240-017-1253-0](https://doi.org/10.1007/s11240-017-1253-0).
- Lisek J, Schauer N, Kopka J et al. Gas chromatography mass spectrometry-based metabolite profiling in plants. *Nat Protoc* 2006;**1**:387–96. doi: [10.1038/nprot.2006.59](https://doi.org/10.1038/nprot.2006.59).



18. Nikhil K, Sharan S, Chakraborty A et al. Role of isothiocyanate conjugate of pterostilbene on the inhibition of MCF-7 cell proliferation and tumor growth in Ehrlich ascitic cell induced tumor bearing mice. *Exp Cell Res* 2014;320:311–28. doi: [10.1016/j.yexcr.2013.10.015](https://doi.org/10.1016/j.yexcr.2013.10.015).
19. Kasibhatla S, Amarante-Mendes GP, Finucane D et al. Acridine Orange/Ethidium bromide (AO/EB) staining to detect apoptosis. *Cold Spring Harb Protoc* 2006;3:pdb.prot4493-pdb.prot4493. doi: [10.1101/pdb.prot4493](https://doi.org/10.1101/pdb.prot4493).
20. Crowley LC, Marfell BJ, Waterhouse NJ. Analyzing cell death by nuclear staining with Hoechst 33342. *Cold Spring Harb Protoc* 2016;9:778–81. doi: [10.1101/pdb.prot087205](https://doi.org/10.1101/pdb.prot087205).
21. Crowley LC, Marfell BJ, Christensen ME et al. Measuring cell death by trypan blue uptake and light microscopy. *Cold Spring Harb Protoc* 2016;7:643–6. doi: [10.1101/pdb.prot087155](https://doi.org/10.1101/pdb.prot087155).
22. Nishio S, Teshima Y, Takahashi N et al. Activation of CaMKII as a key regulator of reactive oxygen species production in diabetic rat heart. *J Mol Cell Cardiol* 2012;52:1103–11. doi: [10.1016/j.yjmcc.2012.02.006](https://doi.org/10.1016/j.yjmcc.2012.02.006).
23. Livak KJ, Schmittgen TD. Analysis of relative gene expression data using real-time quantitative PCR and the 2- $\Delta\Delta$ CT method. *Methods* 2001;25:402–8. doi: [10.1006/meth.2001.1262](https://doi.org/10.1006/meth.2001.1262).
24. Morris GM, Huey R, Lindstrom W et al. AutoDock4 and AutoDockTools4: automated docking with selective receptor flexibility. *J Comput Chem* 2009;30:2785–91. doi: [10.1002/jcc.21256](https://doi.org/10.1002/jcc.21256).
25. Touré BB, Miller-Moslin K, Yusuff N et al. The role of the acidity of N-heteroaryl sulfonamides as inhibitors of Bcl-2 family protein-protein interactions. *ACS Med Chem Lett* 2013;4:186–90. doi: [10.1021/ml300321d](https://doi.org/10.1021/ml300321d).
26. Inoue A, Kikuchi S, Hishiki A et al. A small molecule inhibitor of monoubiquitinated proliferating cell nuclear antigen (PCNA) inhibits repair of interstrand DNA cross-link, enhances DNA double strand break, and sensitizes cancer cells to cisplatin. *J Biol Chem* 2014;289:7109–20. doi: [10.1074/jbc.M113.520429](https://doi.org/10.1074/jbc.M113.520429).
27. Riedl SJ, Li W, Chao Y et al. Structure of the apoptotic protease-activating factor 1 bound to ADP. *Nature* 2005;434:926–33. doi: [10.1038/nature03465](https://doi.org/10.1038/nature03465).
28. Pettersen EF, Goddard TD, Huang CC et al. UCSF chimera - a visualization system for exploratory research and analysis. *J Comput Chem* 2004;25:1605–12. doi: [10.1002/jcc.20084](https://doi.org/10.1002/jcc.20084).
29. Sanlier N, Gencer F. Role of spices in the treatment of diabetes mellitus: a minireview. *Trends Food Sci Technol* 2020;99:441–9. doi: [10.1016/j.tifs.2020.03.018](https://doi.org/10.1016/j.tifs.2020.03.018).
30. Macedo AL, da Silva DPD, Moreira DL et al. Cytotoxicity and selectiveness of Brazilian Piper species towards oral carcinoma cells. *Biomed Pharmacother* 2019;110:342–52. doi: [10.1016/j.biopha.2018.11.129](https://doi.org/10.1016/j.biopha.2018.11.129).
31. Fidy K, Fiedorowicz A, Strz̧dała L et al.  $\beta$ -Caryophyllene and  $\beta$ -Caryophyllene oxide—natural compounds of anticancer and analgesic properties. *Cancer Med* 2016;5:3007–17. doi: [10.1002/cam4.816](https://doi.org/10.1002/cam4.816).
32. Pei K, Ou J, Huang J et al. P-Coumaric acid and its conjugates: dietary sources, pharmacokinetic properties and biological activities. *J Sci Food Agric* 2016;96:2952–62. doi: [10.1002/jsfa.7578](https://doi.org/10.1002/jsfa.7578).
33. Derosa G, Maffioli P, Sahebkar A. Piperine and its role in chronic diseases. In: Gupta S, Prasad S, Aggarwal B. (eds). *Anti-inflammatory Nutraceuticals and chronic diseases. Advances in Experimental Medicine and Biology*. 928:173–84, 2016. doi: [10.1007/978-3-319-41334-1\\_8](https://doi.org/10.1007/978-3-319-41334-1_8).
34. Arur S, Uche UE, Rezaul K et al. Annexin I is an endogenous ligand that mediates apoptotic cell engulfment. *Dev Cell* 2003;4:587–98. doi: [10.1016/S1534-5807\(03\)00090-X](https://doi.org/10.1016/S1534-5807(03)00090-X).
35. Greenshields AL, Doucette CD, Sutton KM et al. Piperine inhibits the growth and motility of triple-negative breast cancer cells. *Cancer Lett* 2015;357:129–40. doi: [10.1016/j.canlet.2014.11.017](https://doi.org/10.1016/j.canlet.2014.11.017).
36. Lavrik I, Golks A, Krammer PH. Death receptor signaling. *J Cell Sci* 2005;118:265–7. doi: [10.1242/jcs.01610](https://doi.org/10.1242/jcs.01610).
37. Li J, Yuan J. Caspases in apoptosis and beyond. *Oncogene* 2008;27:6194–06. doi: [10.1038/onc.2008.297](https://doi.org/10.1038/onc.2008.297).
38. Vinaya K, Kavitha CV, Chandrappa S et al. Synthesis and antileukemic activity of novel 4-(3-(Piperidin-4-yl) propyl)Piperidine derivatives. *Chem Biol Drug Des* 2011;78:622–30. doi: [10.1111/j.1747-0285.2011.01184.x](https://doi.org/10.1111/j.1747-0285.2011.01184.x).
39. Gariboldi MB, Ravizza R, Petterino C et al. Study of *in vitro* and *in vivo* effects of the piperidine nitroxide Tempol - a potential new therapeutic agent for gliomas. *Eur J Cancer* 2003;39:829–37. doi: [10.1016/S0959-8049\(02\)00742-6](https://doi.org/10.1016/S0959-8049(02)00742-6).
40. Zhao Y, Luo Q, Mo J et al. Metformin in combination with JS-K inhibits growth of renal cell carcinoma cells via reactive oxygen species activation and inducing DNA breaks. *J Cancer* 2002;11:3701–12. doi: [10.7150/jca.36372](https://doi.org/10.7150/jca.36372).
41. Dasari S, Bakthavachalam V, Chinnapaka S, Samy ALPA et al. Neferine, an alkaloid from lotus seed embryo targets HeLa and SiHa cervical cancer cells via pro-oxidant anticancer mechanism. *Phytother Res* 2020;34:1–19. doi: [10.1002/ptr.6687](https://doi.org/10.1002/ptr.6687).
42. Lee WYW, Liu KWK, Yeung JHK. Reactive oxygen species-mediated kinase activation by dihydrotanshinone in tanshinones-induced apoptosis in HepG2 cells. *Cancer Lett* 2009;285:46–57. doi: [10.1016/j.canlet.2009.04.040](https://doi.org/10.1016/j.canlet.2009.04.040).
43. Moon D-O, Kim M-O, Kang S-H et al. Sulforaphane suppresses TNF- $\alpha$ -mediated activation of NF- $\kappa$ B and induces apoptosis through activation of reactive oxygen species-dependent caspase-3. *Cancer Lett* 2009;274:132–42. doi: [10.1016/j.canlet.2008.09.013](https://doi.org/10.1016/j.canlet.2008.09.013).
44. Liang JR, Yang H. Ginkgolic acid (GA) suppresses gastric cancer growth by inducing apoptosis and suppressing STAT3/JAK2 signaling regulated by ROS. *Biomed Pharmacother* 2020;125:109585. doi: [10.1016/j.biopha.2019.109585](https://doi.org/10.1016/j.biopha.2019.109585).
45. Liu ZH, Yang CX, Zhang L et al. Baicalein, as a prooxidant, triggers mitochondrial apoptosis in MCF-7 human breast cancer cells through mobilization of intracellular copper and reactive oxygen species generation. *Onco Targets Ther* 2019;12:10749–61. doi: [10.2147/OTT.S222819](https://doi.org/10.2147/OTT.S222819).
46. Paunesku T, Mittal S, Protić M et al. Proliferating cell nuclear antigen (PCNA): ringmaster of the genome. *Int J Radiat Biol* 2001;77:1007–21. doi: [10.1080/09553000110069335](https://doi.org/10.1080/09553000110069335).
47. Guedes IA, de Magalhães CS, Dardenne LE. Receptor-ligand molecular docking. *Biophys Rev* 2014;6:75–87. doi: [10.1007/s12551-013-0130-2](https://doi.org/10.1007/s12551-013-0130-2).